Influence of initiators on the sintering discolouration of PTFE

W.V. Venner, G.J. Puts, P.L. Crouse

Department of Chemical Engineering, Faculty of Engineering, Built Environment and IT, University of Pretoria

SUPPORTING INFORMATION

1. *Ab initio* calculations

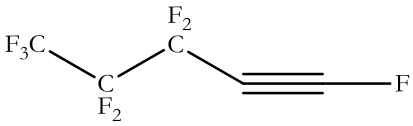

Fig. 1. Structure of the proposed terminal alkyne group used for ab initio calculations [1]. The structure was modelled with only 3 carbon backbone atoms in the chain to limit calculation time. Adding more would have constituted a better representation of a PTFE chain, but would have significantly increased calculation time. It is believed that the modelled compound provided an accurate depiction for the purpose of identifying end groups.

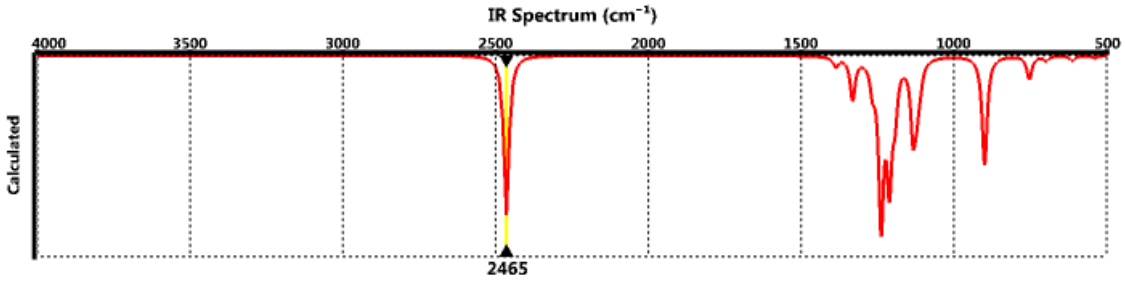

Fig. 2. Predicted IR spectra of the proposed terminal alkyne group, according to ab initio calculations [1] It corresponds very well with the frequencies predicted for these groups with the help of the publication by Socrates [2]. It shows a very strong band at 2465 cm^{-1} in the IR spectrum which is assigned to the terminal C≡C group.

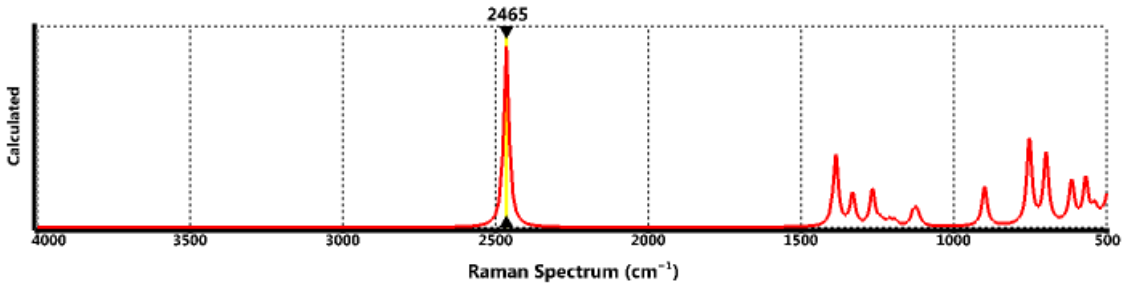

Fig. 3. Predicted Raman spectra of the proposed terminal alkyne group, according to ab initio calculations [1]. The very large peak at 2465 cm^{-1} is only slightly higher than the estimated value of ~2450 cm^{-1}. The higher than expected frequency is likely because of the highly

electronegative nature of the F atom. There is also a medium intensity peak at 612 cm^{-1} which coincides with the literature range of 500 – 800 cm^{-1}.

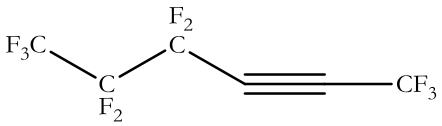

Fig. 4. Structure of the proposed inner (non-terminal) alkyne group for ab initio calculations [1].

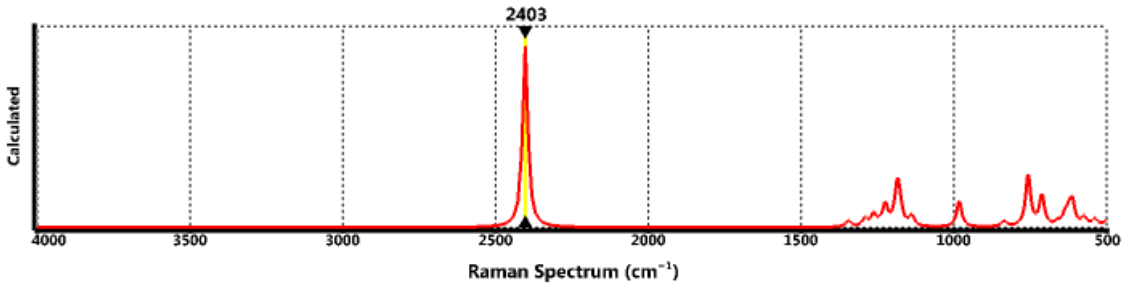

Fig. 5. Predicted Raman spectra of the proposed inner alkyne group, according to ab initio calculations [1]. The calculated Raman spectra coincides with the values predicted with the help of Socrates. The intense peak at 2403 cm^{-1}, as well as the less intense peak at ~600 cm^{-1}, fall into the predicted ranges.

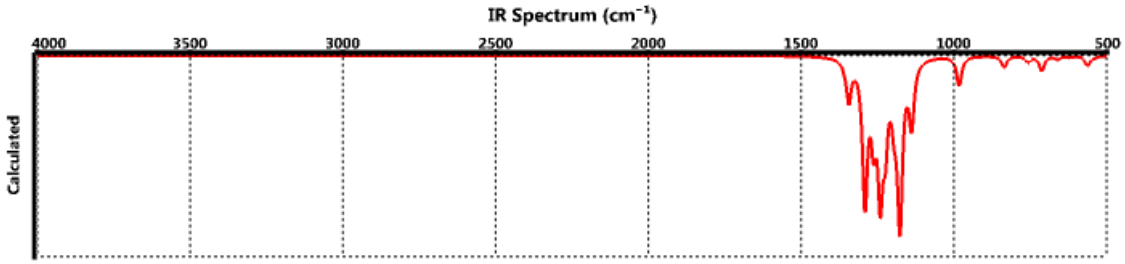

Fig. 6. Predicted IR spectra of the proposed inner alkyne group, according to ab initio calculations [1]. It shows the clear absence of any band in the region of ~2450 cm^{-1}. This is because of the inner position of the C≡C bond which lessens the intensity of the band in the IR spectrum.

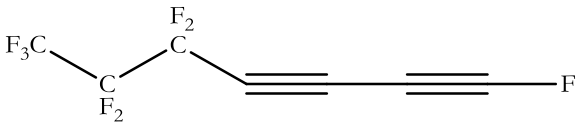

Fig. 7. Structure of the proposed double alkyne group for ab initio calculations.

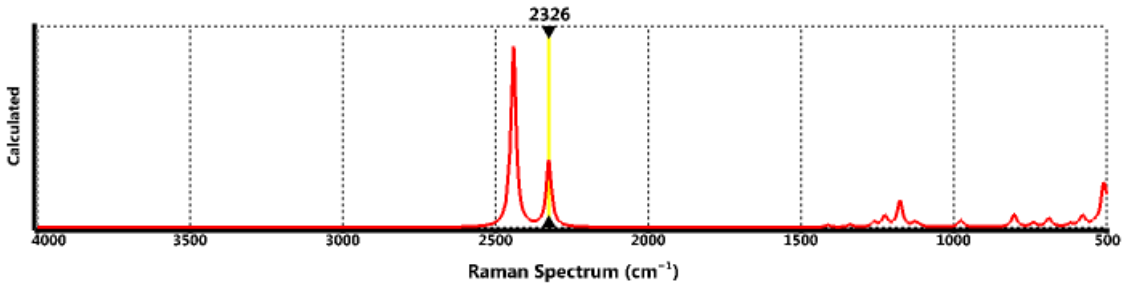

Fig. 8. Predicted Raman spectra of the proposed double alkyne group, according to ab initio calculations. Calculated Raman spectra shows a very intense peak at ~2440 cm^{-1}, which is due to the C≡C stretching vibration. This coincides well with the value predicted with the help of Socrates. However, there is another well defined peak at 2326 cm^{-1}, which is likely due to an overtone/combination band enhanced by Fermi resonance, due to the disubstituted nature of the alkyne.

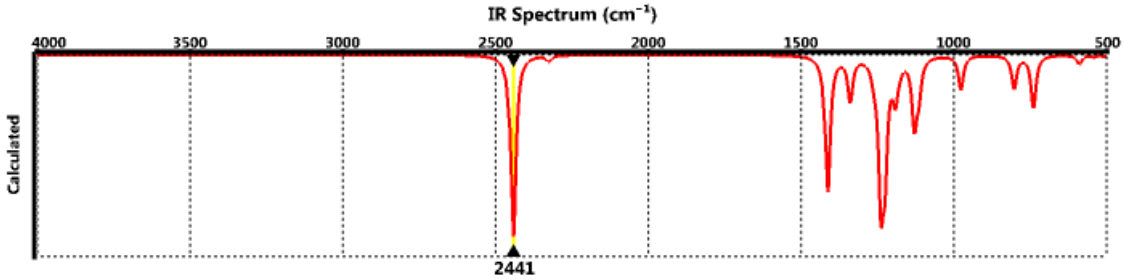

Fig. 9. Predicted IR spectra of the proposed double alkyne group, according to ab initio calculations. Similarly to the IR spectra of the terminal alkyne group, the double alkyne group shows a very strong peak at 2441 cm^{-1}, which indicates the terminal C≡C bond.

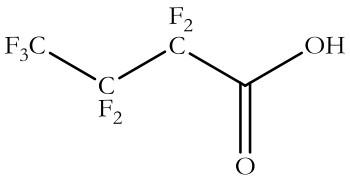

Fig. 10. Structure of the proposed perfluorocarboxylic acid end group for ab initio calculations

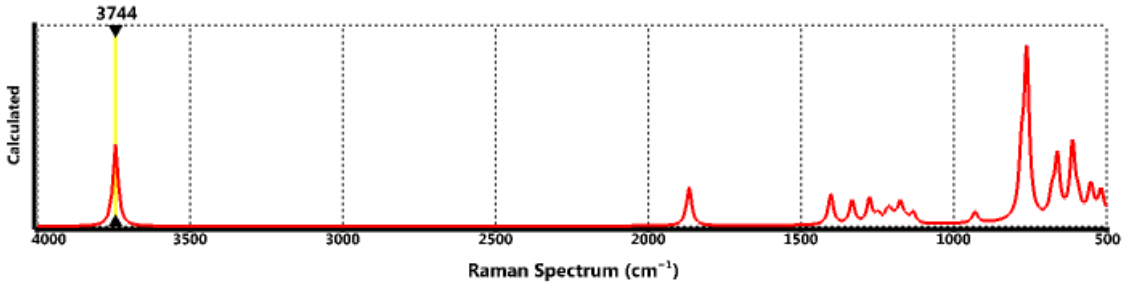

Fig. 11. Predicted Raman spectra of the proposed prefluorocarboxylic acid end group, according to ab initio calculations. The sharp, medium intensity band at ~1900 cm^{-1} is likely due to the C=O stretching vibration which has been shifted higher than normal (~1700 cm^{-1}) due to the electronegative fluorine atoms. Once again the sharp bands at ~750 cm^{-1} are in a region that is densely populated by PTFE vibrations and will therefore be very difficult to identify in sampled spectra. The band at 3744 cm^{-1} is unexpected and unassigned in Socrates and Pianca [3].

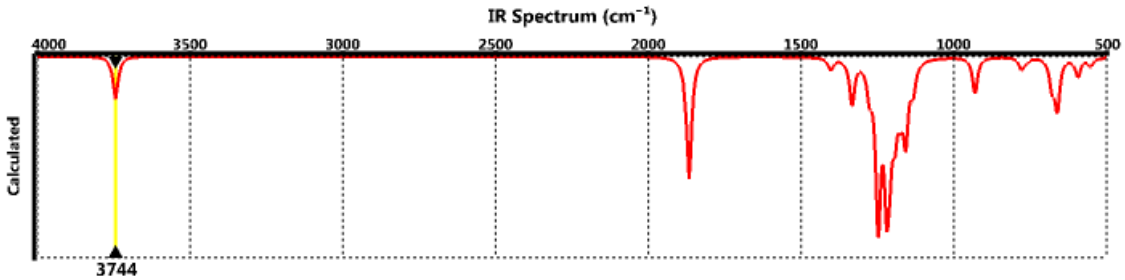

Fig. 12. Predicted IR spectra of the proposed prefluorocarboxylic acid end group, according to ab initio calculations. It can be seen that the broad band at 3300 – 2500 cm^{-1} due to hydrogen bonding of the OH groups reported by Socrates is completely absent. Though this is likely because the compound was only modelled as a single molecule and therefore no hydrogen bonding between molecules could occur. Socrates reports that the C=O

group absorbs very strongly in the region ~1720 cm^{-1} and this frequency is heightened by electronegative substituents. It is unclear what the sharp, medium intensity band at 3744 cm^{-1} indicates.

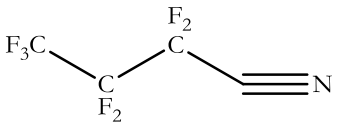

Fig. 13. Structure of the proposed perfluoronitrile end group for ab initio calculations.

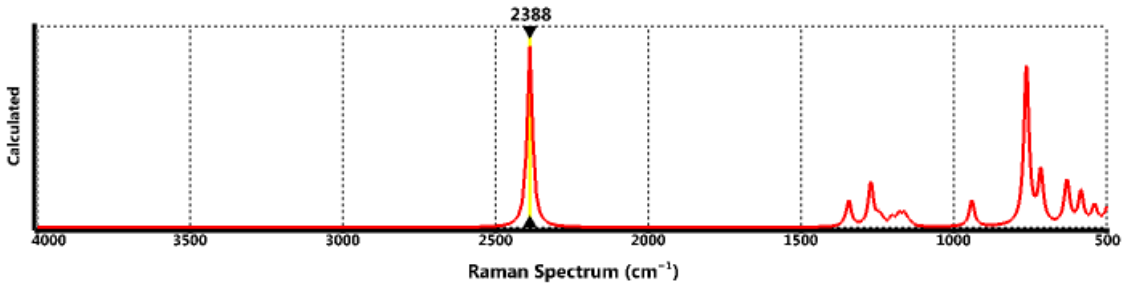

Fig. 14. Predicted Raman spectra of the proposed prefluoronitrile end group, according to ab initio calculations. The calculated Raman spectra agrees with the predicted sharp band in the region of ~2250 cm^{-1}, though this band is at a somewhat higher frequency due to the highly electronegative nature of the nitrile group's substituents. Socrates also reports medium bands in the region ~560 cm^{-1}. The band at ~750 cm^{-1} is not assigned to any stretching vibration of a nitrile group by Socrates.

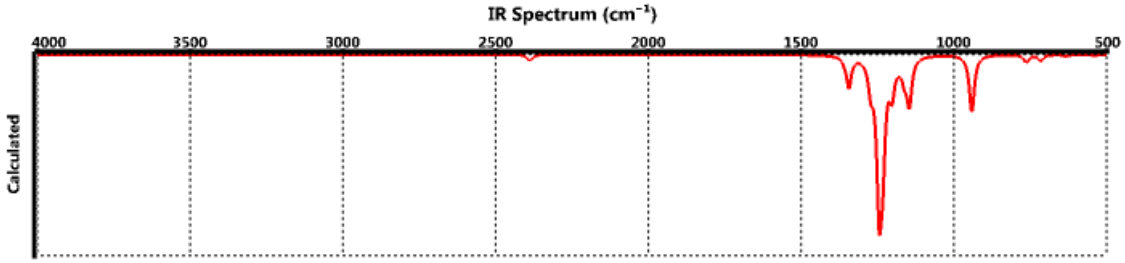

Fig. 15. Predicted IR spectra of the proposed prefluoronitrile end group, according to ab initio calculations. The sharp absorption band predicted by Socrates at ~2250 cm^{-1} is of a very

weak intensity and at a higher frequency closer to ~2400 cm^{-1}. The higher frequency and weak intensity are expected due to the highly electronegative nature of the nitrile group's substituents. The sharp bands all occur in the same region as PTFE's strong structural vibrational bands. This made identification when interpreting the results very difficult.

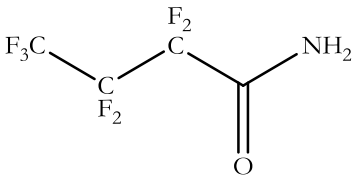

Fig. 16. Structure of the proposed perfluoro amide end group for ab initio calculations.

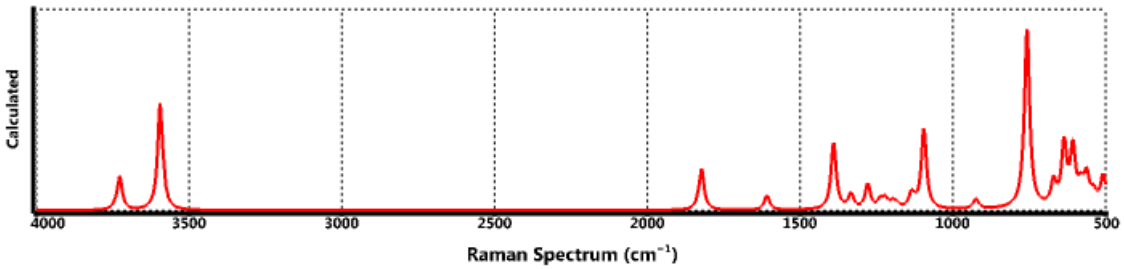

Fig. 17. Predicted Raman spectra of the proposed prefluoro amide end group, according to ab initio calculations. The calculated Raman spectra is somewhat different than the spectra predicted by Socrates and Pianca. The two bands at ~1768 and 1587 cm^{-1} are present and of weak intensity, as expected. However, the two bands that were predicted at 3555 and 3438 cm^{-1} seems to have shifted to significantly higher frequencies of ~3700 and 3600 cm^{-1}. This could be because of the electronegative nature of the fluorine atoms shifting the frequencies higher.

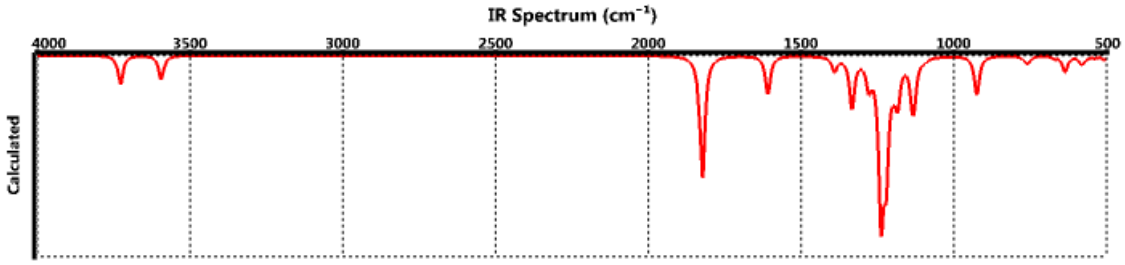

Fig. 18. Predicted IR spectra of the proposed prefluoro amide end group, according to ab initio calculations.

2. Photos of pressed PTFE discs, before and after sintering

APS initiated PTFE

Exp #	Unsintered	Sintered 2 min	30 min
1			n/a
2			
3			
4			

5			n/a
6		n/a	n/a
7			
8			
9			
10			
11			
12			n/a

13			n/a
14			
15			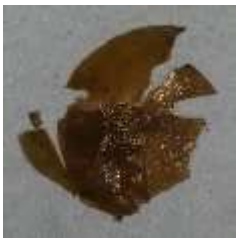
16			
17		n/a	
18		n/a	
Commercial PTFE		n/a	

K_2CO_3		n/a	

Photo-initiated PTFE samples

Experiment	Unsintered	Sintered 5 min	Sintered 30 min
H_2O_2 in sunlight #1		n/a	
H_2O_2 in sunlight #2			
APS in sunlight		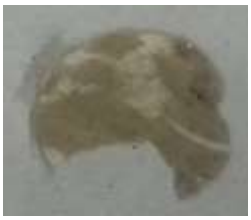	
H_2O_2 exposed to Vis, IR, UV			n/a
H_2O_2 exposed to Vis, IR	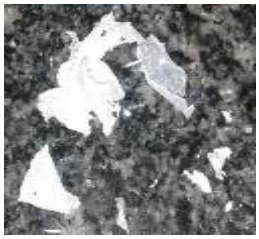		n/a

H_2O_2 exposed to IR, UV		n/a	n/a
H_2O_2 exposed to UV, Vis		n/a	n/a

Thermally initiated PTFE samples

Initiator	Unsintered	Sintered 30 min
1% DTBP		
10% DTBP		
30% DTBP		
1% $KMnO_4$		

10% $KMnO_4$		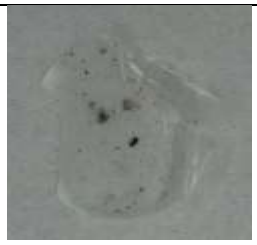
30% $KMnO_4$		
Sodium persulfate		
30% $KMnO_4$ after additional 24 h wash.	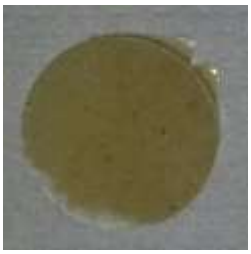	

3. FTIR spectra

3.1 Unprocessed PTFE samples

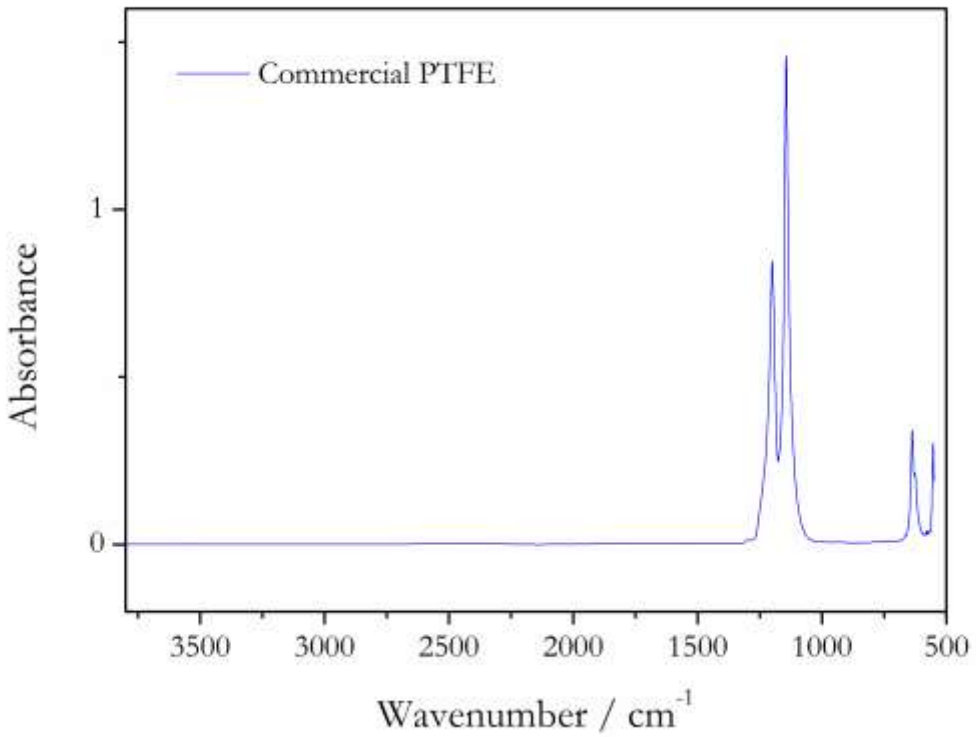

Fig. 19. ATR FTIR spectrum of commercial PTFE obtained from DuPont. It only shows bands associated with the structure of PTFE. No other bands, especially bands that could indicate the end groups of the PTFE chains, are visible. This is likely because ATR FTIR spectroscopy only penetrates approximately 2 µm into the particle, which leads to reduced sensitivity.

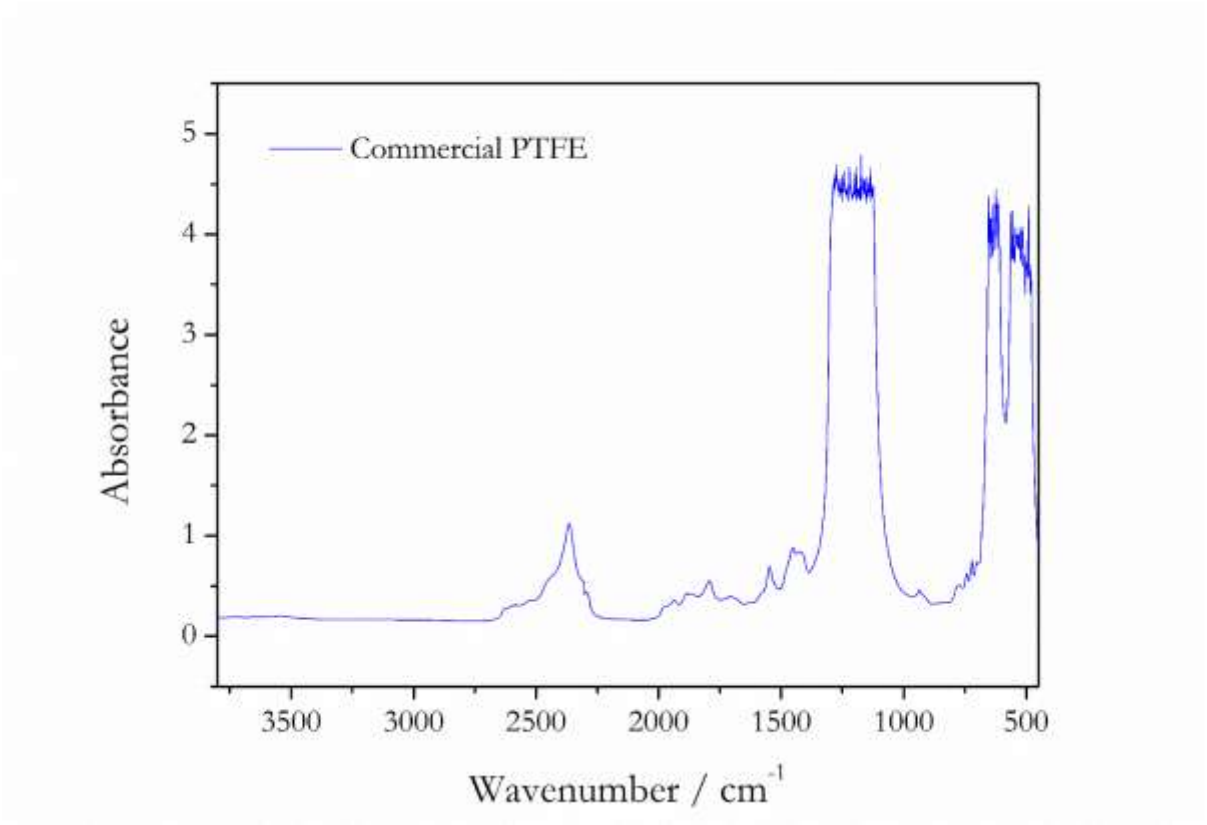

Fig. 20. Transmission FTIR spectra of commercial PTFE, which provides much more detail than the ATR FTIR measurement. According to Socrates, PTFE has strong absorptions, because of the CF_2 repeating units, in the region 1250 – 1100 cm^{-1} and at ~2400 cm^{-1} because of. the overtone of the CF_2 stretching vibration [4].

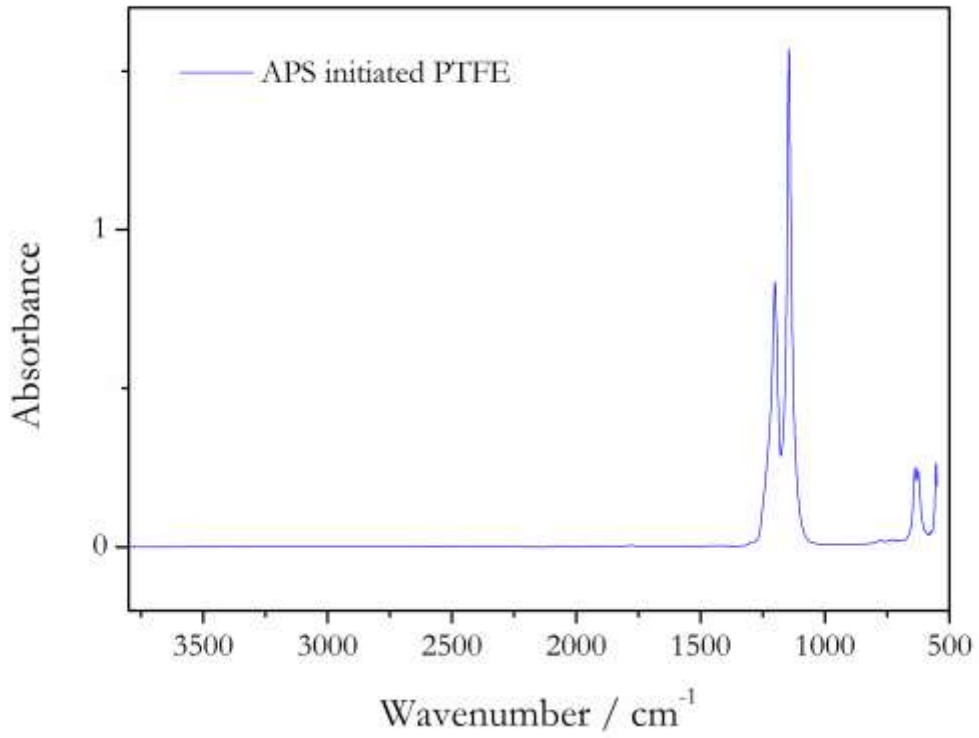

Fig. 21. ATR FTIR spectrum of APS initiated PTFE, experiment APS-6. Similarly to the ATR FTIR of the commercial sample, it does not show any detail. Transmission FTIR measurement were used from this point onward.

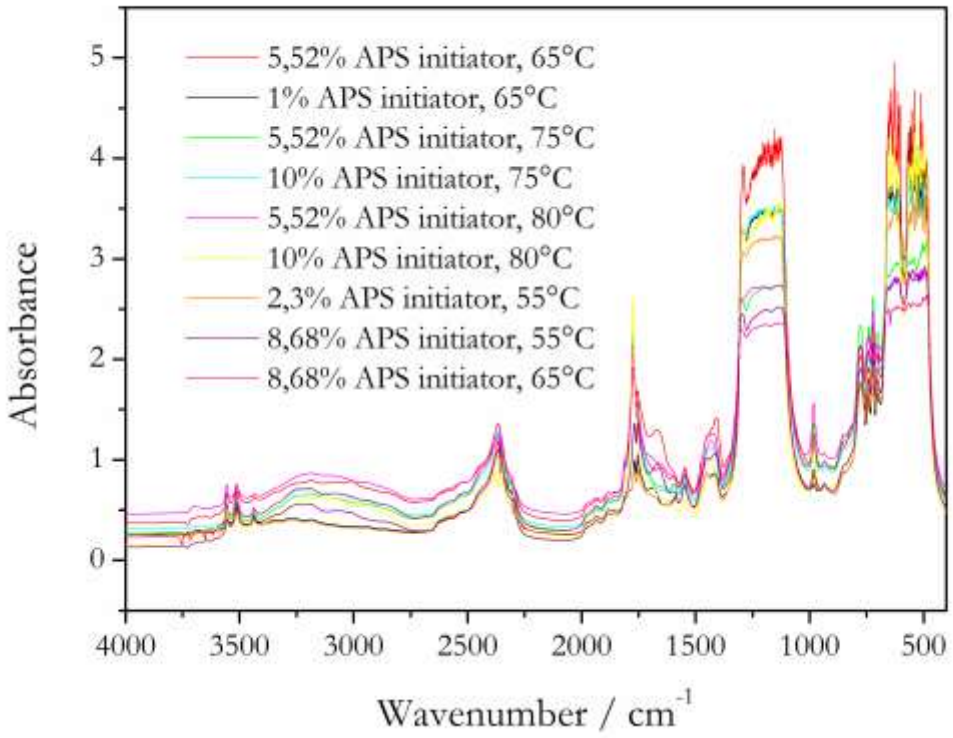

Fig. 22. Overlaid transmission FTIR spectra of the APS-initiated PTFE experiments. The spectra of the APS initiated samples was similar as expected, even though different initiator concentrations were used.

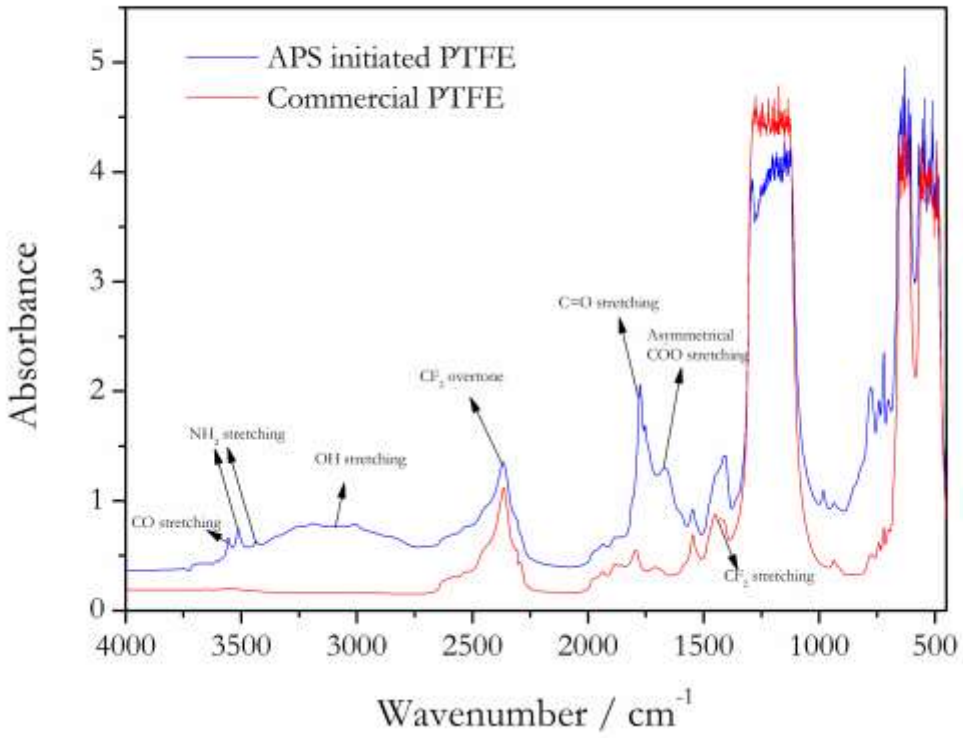

Fig. 23. Overlaid spectra of produced PTFE initiated by APS and commercial PTFE (DuPont). The APS initiated PTFE was of a lower molecular weight than the commercial sample, which accounted for the difference in the peak heights of the structural signals. The other differences in the spectra were attributed to different end groups in the polymers.

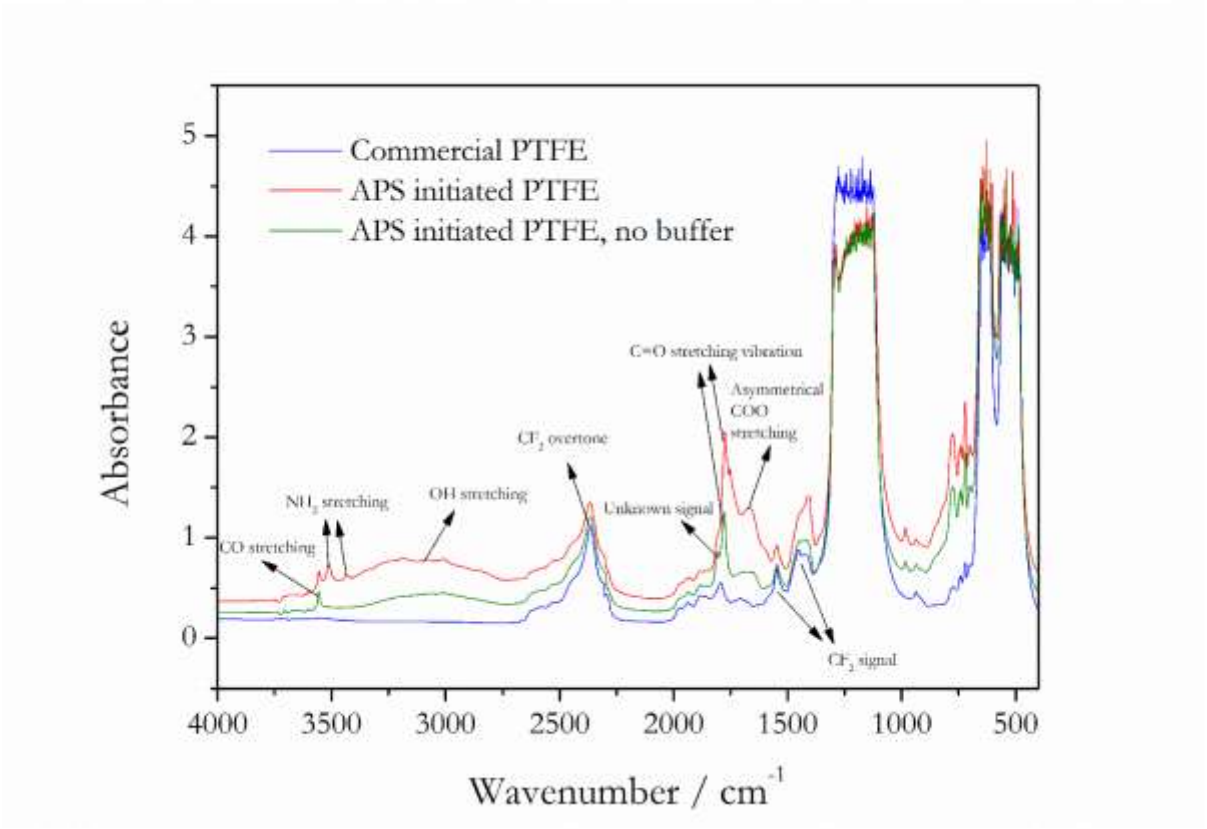

Fig. 24. Overlaid transmission FTIR spectra of PTFE initiated by APS, with and without buffering agents. The use of the same initiator but sans a different buffering agent clearly had an effect on the end-groups that formed in the polymer.

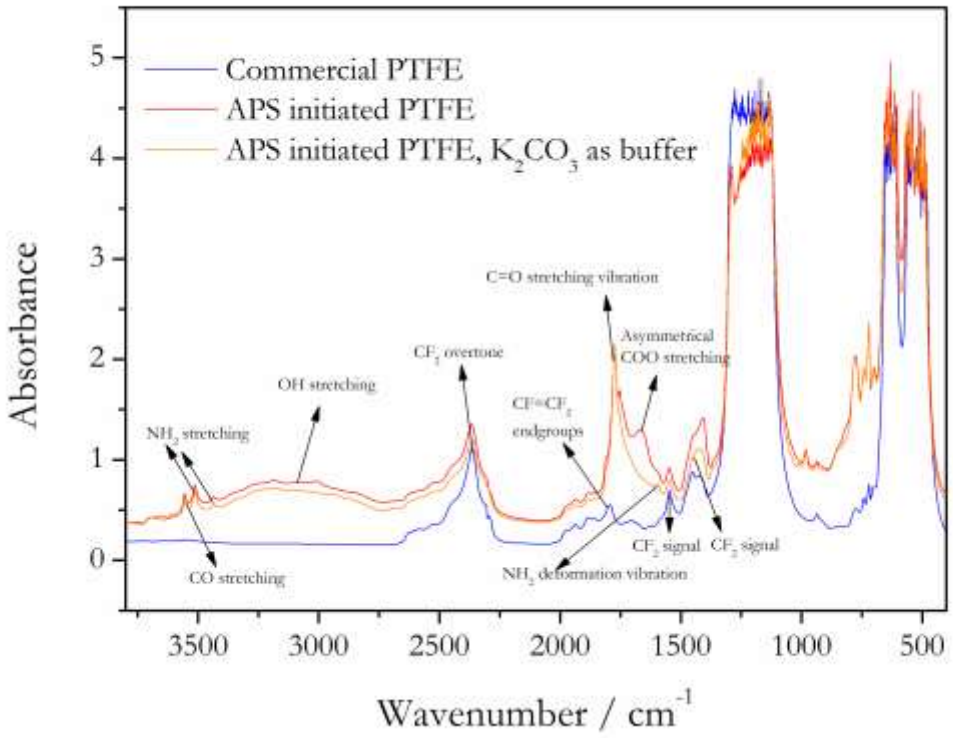

Fig. 25. Overlaid transmission FTIR spectra of PTFE initiated by APS with borax and K_2CO_3 as buffering agents. It is clear the in-house produced PTFE samples have very similar spectra, though there is a signal absent at ~1600 cm^{-1} in the sample that used the different buffering agent. Both differ significantly from the commercial sample.

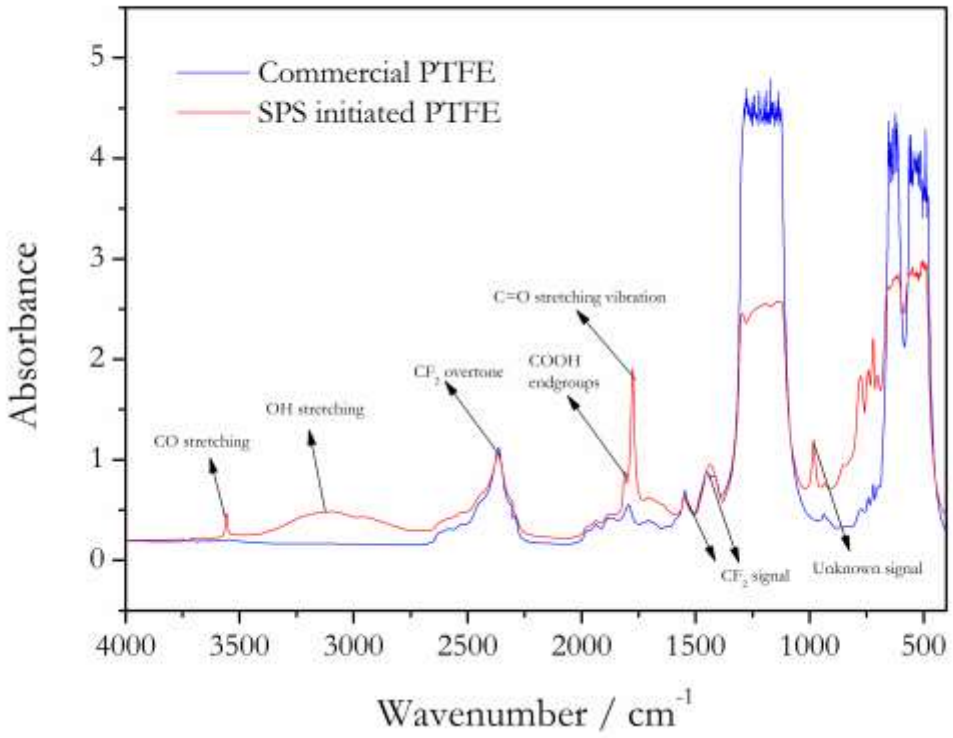

Fig. 26. Overlaid transmission FTIR spectra of PTFE initiated with sodium persulfate. The SPS sample also had multiple termination modes, evidenced by the spectra showing a high concentration of carboxylic end groups and smaller concentration of carboxylic salt end groups.

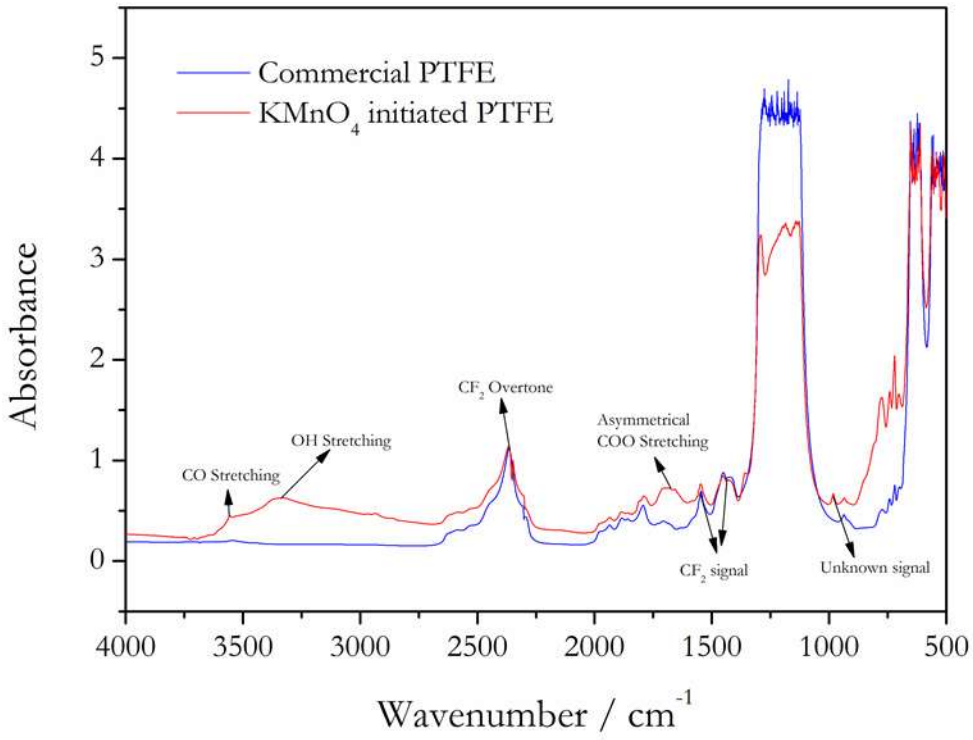

Fig. 27. Overlaid transmission FTIR spectra of PTFE initiated with potassium. permanganate. The spectra indicates that the potassium permanganate initiated PTFE sample is similar to the commercial sample, with the exception being some evidence of OH end groups.

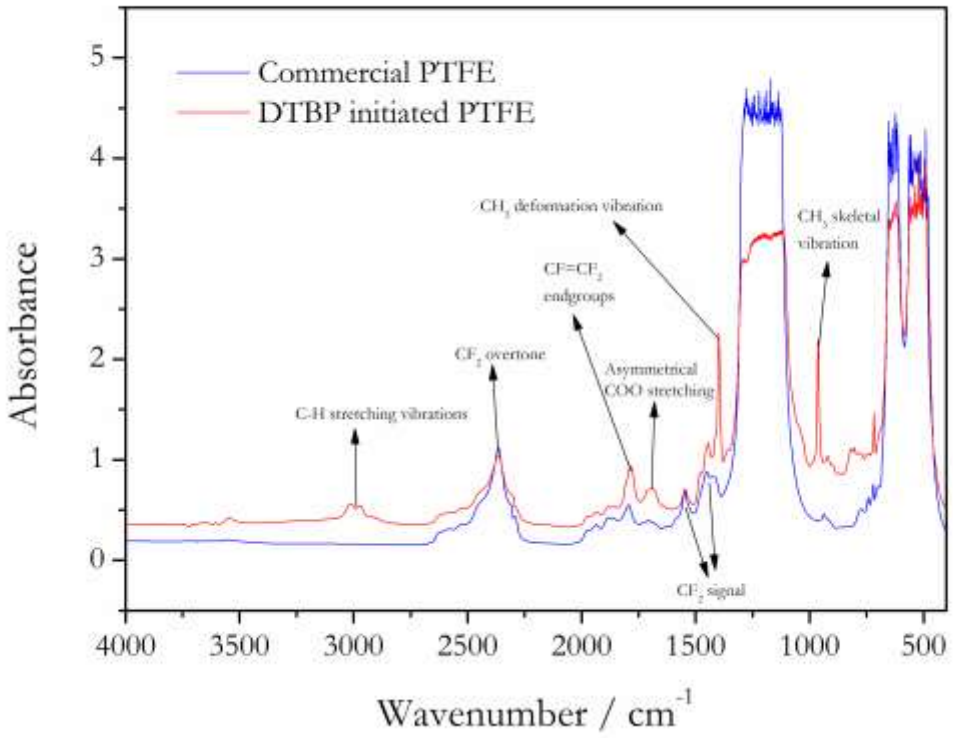

Fig. 28. Overlaid transmission FTIR spectra of PTFE initiated with DTBP. The spectra indicates the presence of tertiary butyl end groups and the absence of carboxylic and carboxylic salt end groups.

3.2 Processed PTFE samples

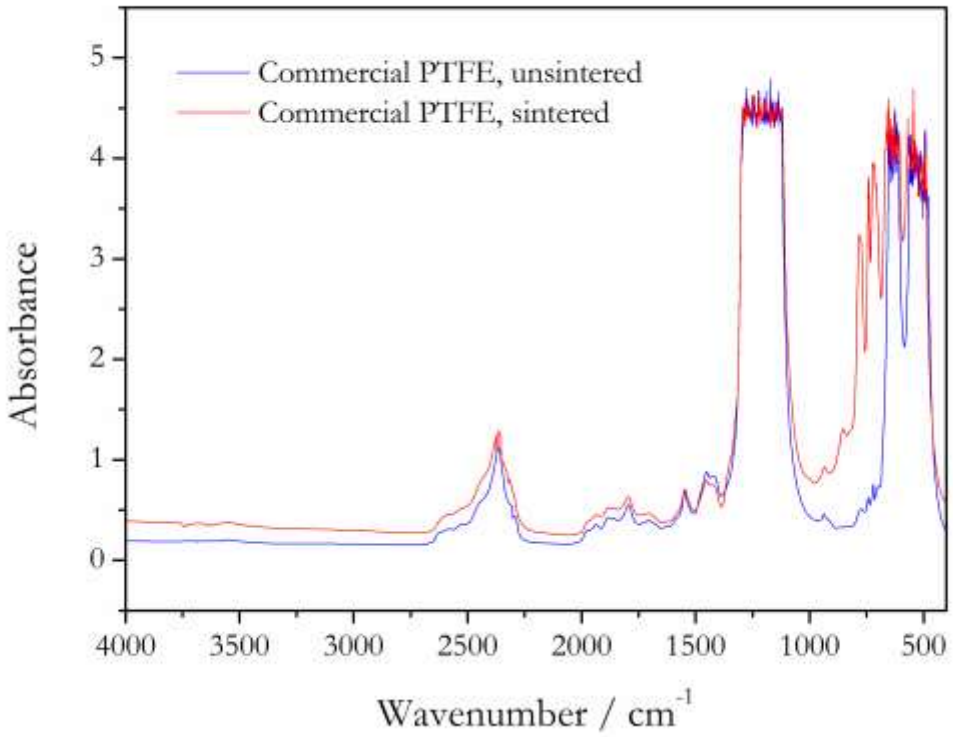

Fig. 29. Transmission FTIR spectra of unsintered and sintered commercial PTFE. The structure of the commercial PTFE sample did not change upon sintering, except for an increase in crystallinity.

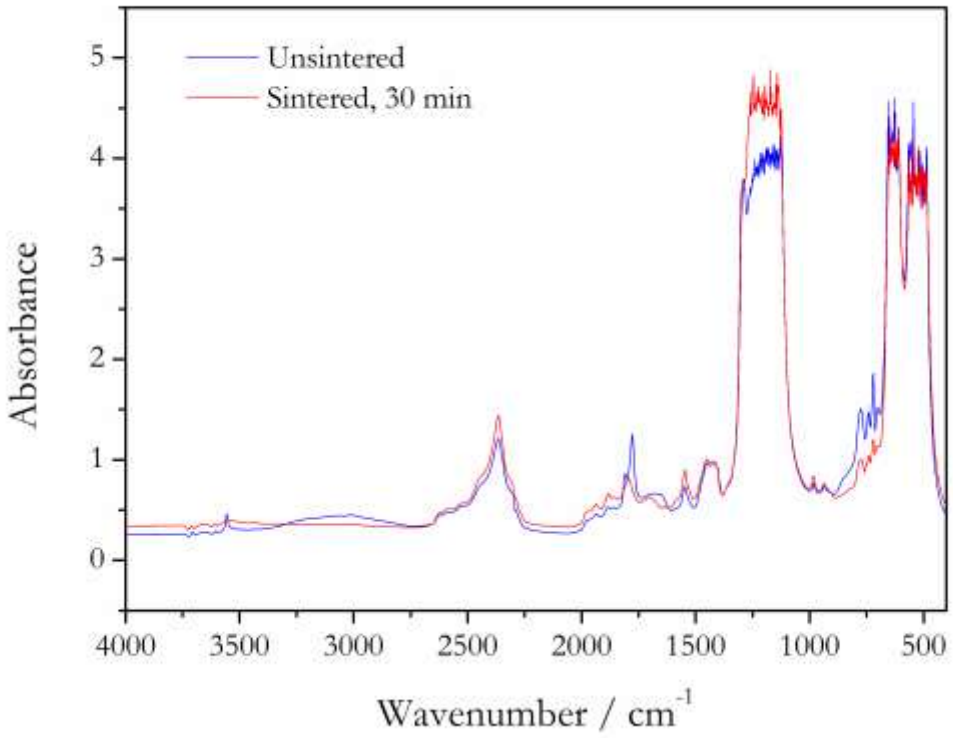

Fig. 30. Overlaid spectra of APS initiated PTFE with no buffer, pre- and post-sintering. The structure is largely unchanged after sintering, except for the decomposition of COOH groups to COF groups.

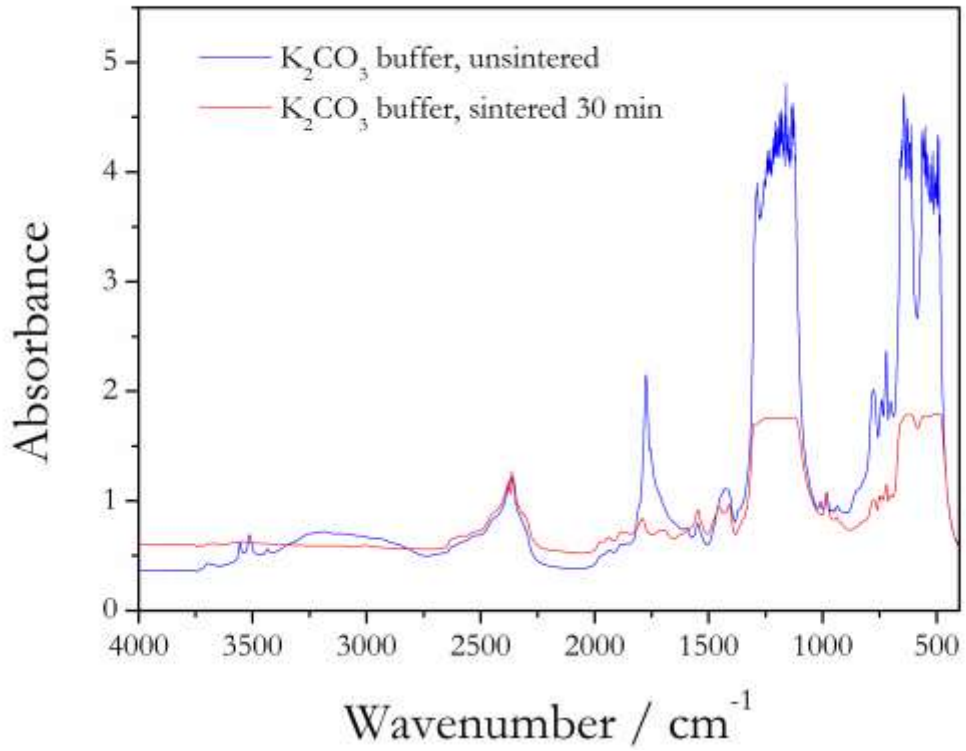

Fig. 31. Overlaid spectra of APS initiated PTFE where K_2CO_3 was used as buffer instead of borax, pre- and post-sintering. It indicates COOH and $CONH_2$ end-groups were eliminated during sintering.

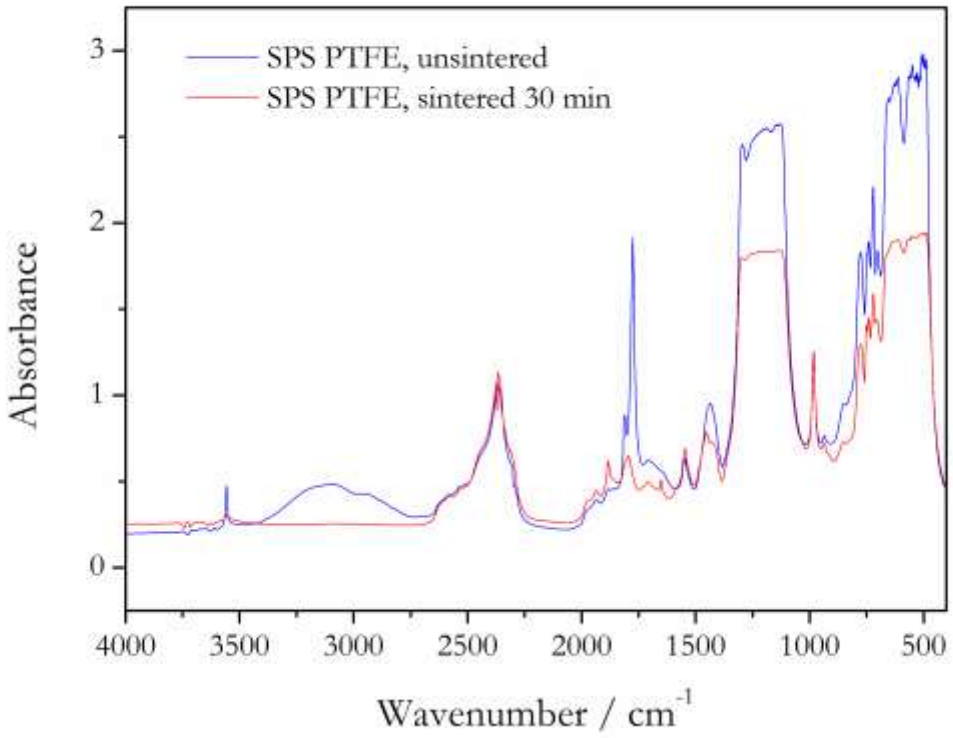

Fig. 32. Overlaid spectra of sodium persulfate initiated samples, before and after sintering. It indicates elimination of carboxylic end-groups and the formation of acyl fluoride groups.

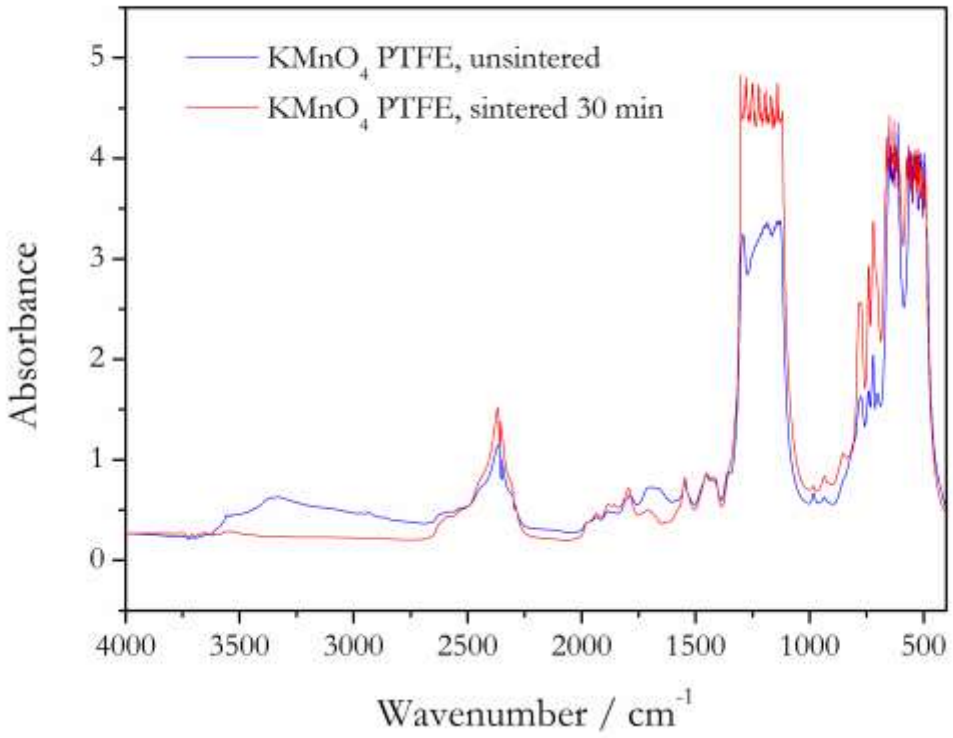

Fig. 33. Overlaid spectra of 10% $KMnO_4$ initiated samples, pre- and post-sintering. The sample is largely unchanged after sintering, except for the reduction of the concentration of OH end-groups.

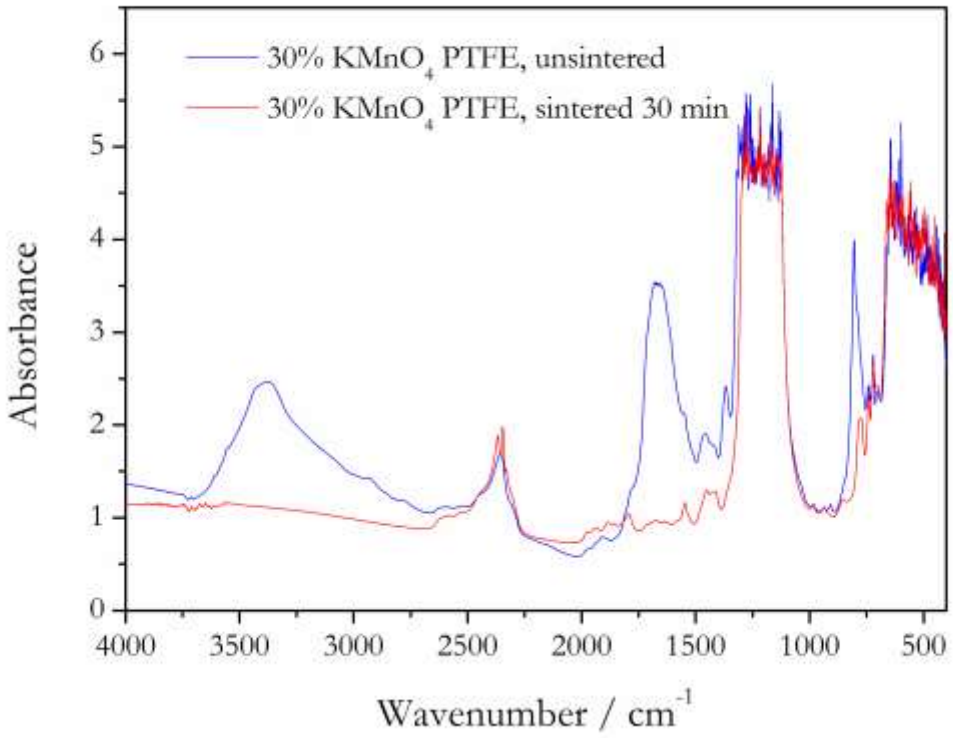

Fig. 34. Overlaid spectra of 30% $KMnO_4$ initiated samples, pre- and post-sintering. This sample also shows reduction of the concentration of OH groups. This sample showed the most discolouration.

4. Raman spectra

4.1 Unprocessed PTFE samples

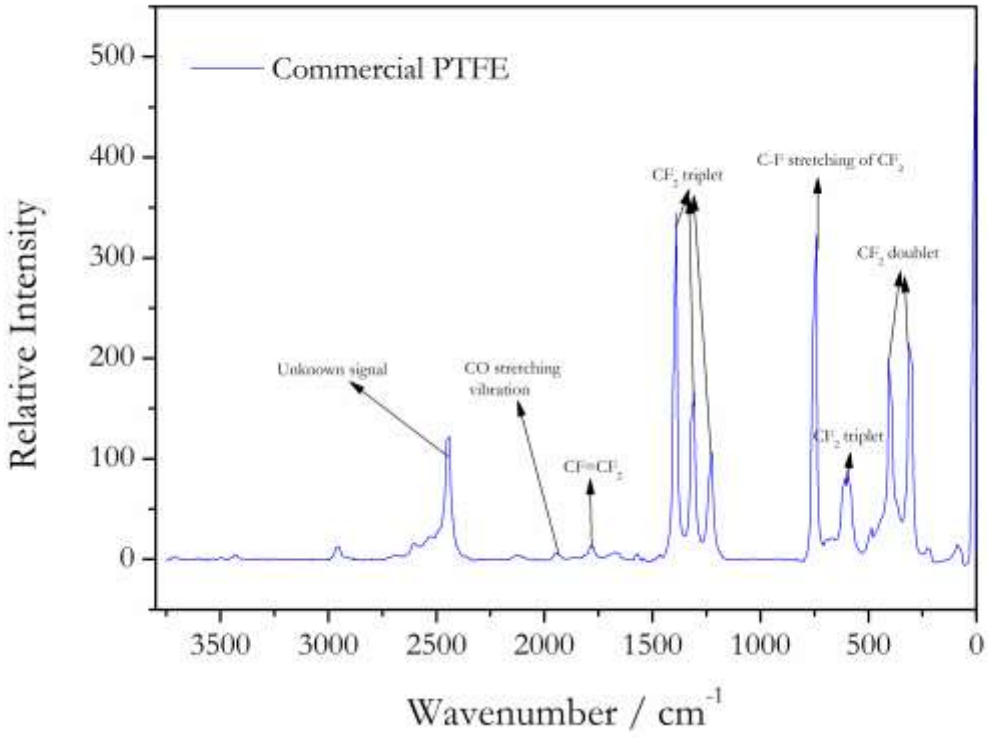

Fig. 35. Raman Spectrum of Commercial PTFE

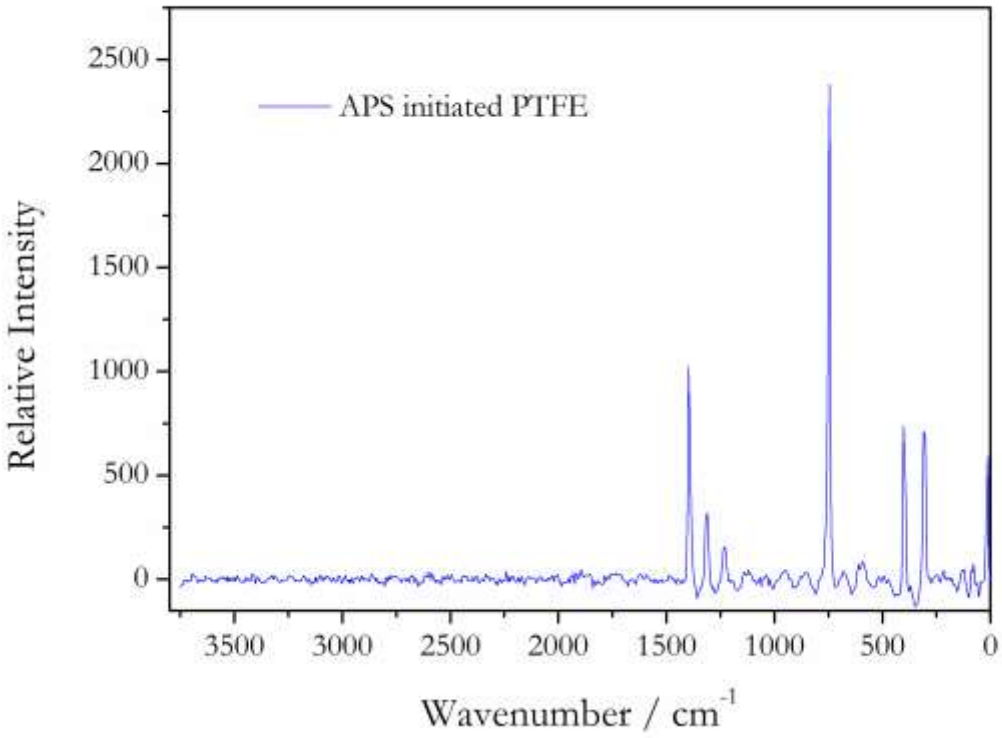

Fig. 36. Raman spectrum of APS initiated PTFE. The APS initiated PTFE samples proved troublesome when it came to collecting Raman spectra. Most of the spectra were poorly defined. It is believed this was because of fluorescence of the samples.

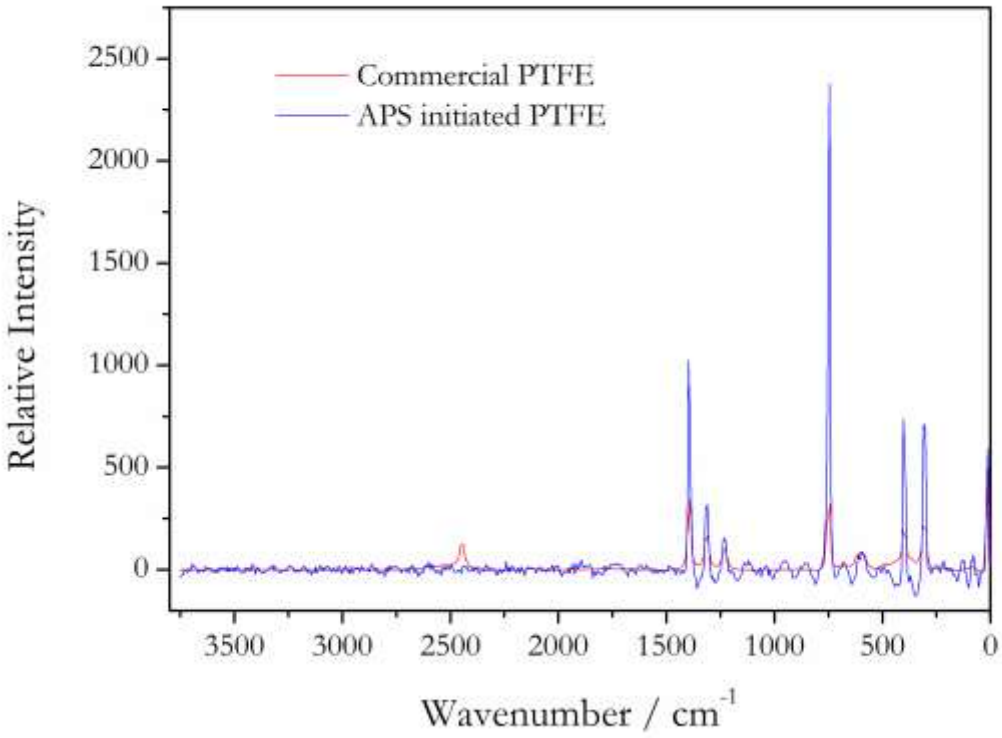

Fig. 37. Overlaid Raman spectra of APS initiated PTFE and commercial PTFE. No peaks indicating end groups are apparent. This could be because the intensity of the structural peaks is so high, that relative to them the end group peaks are all but invisible.

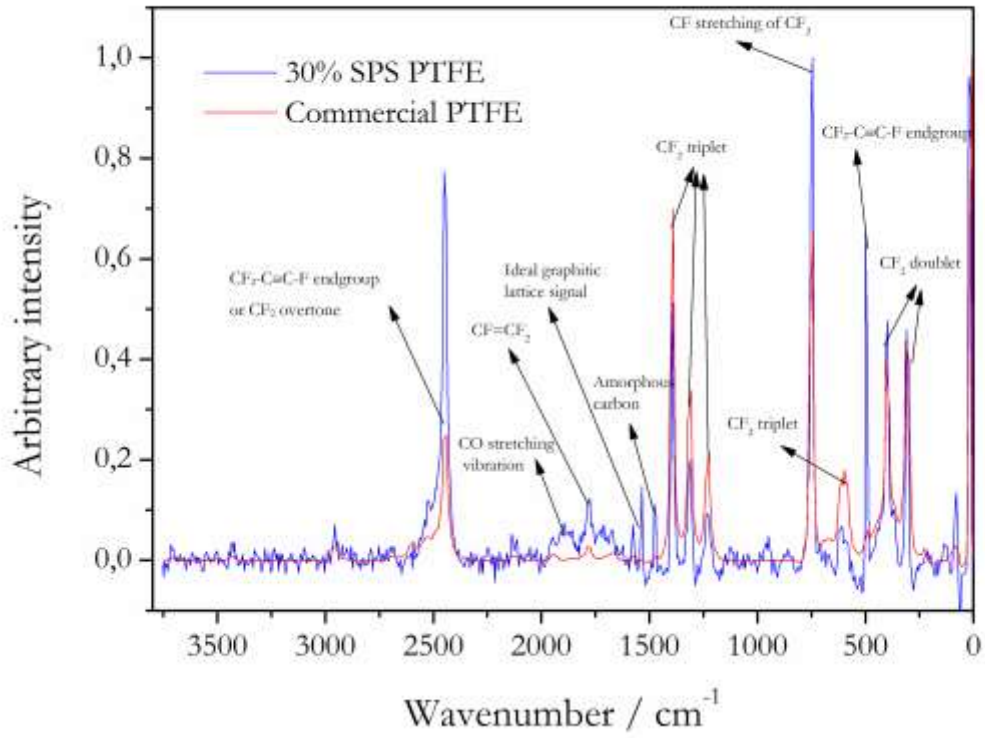

Fig. 38. Overlaid Raman spectra of SPS initiated PTFE and commercial PTFE. The SPS initiated PTFE possesses all the same PTFE structural peaks as the commercial sample, albeit in a lower intensity. The lower intensity can be attributed to the lower molecular weight of the SPS initiated sample.

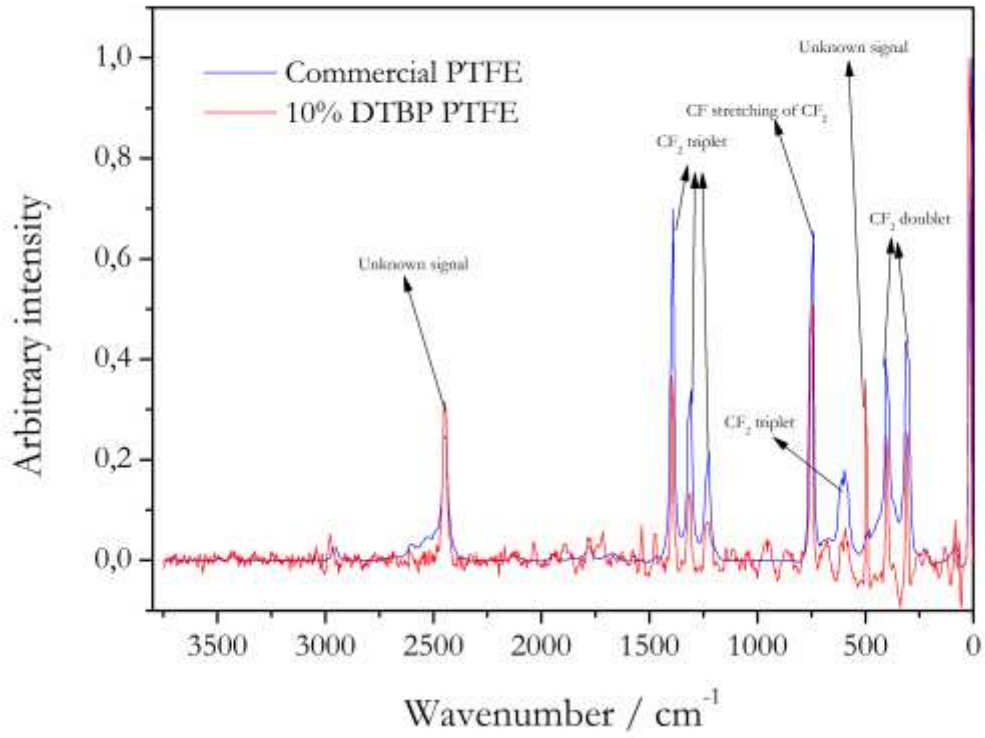

Fig. 39. Overlaid Raman spectra of DTBP initiated PTFE and commercial PTFE. The DTBP initiated PTFE possesses all the same PTFE structural peaks as the commercial sample, albeit in a lower intensity. The lower intensity can be attributed to the lower molecular weight of the DTBP initiated sample.

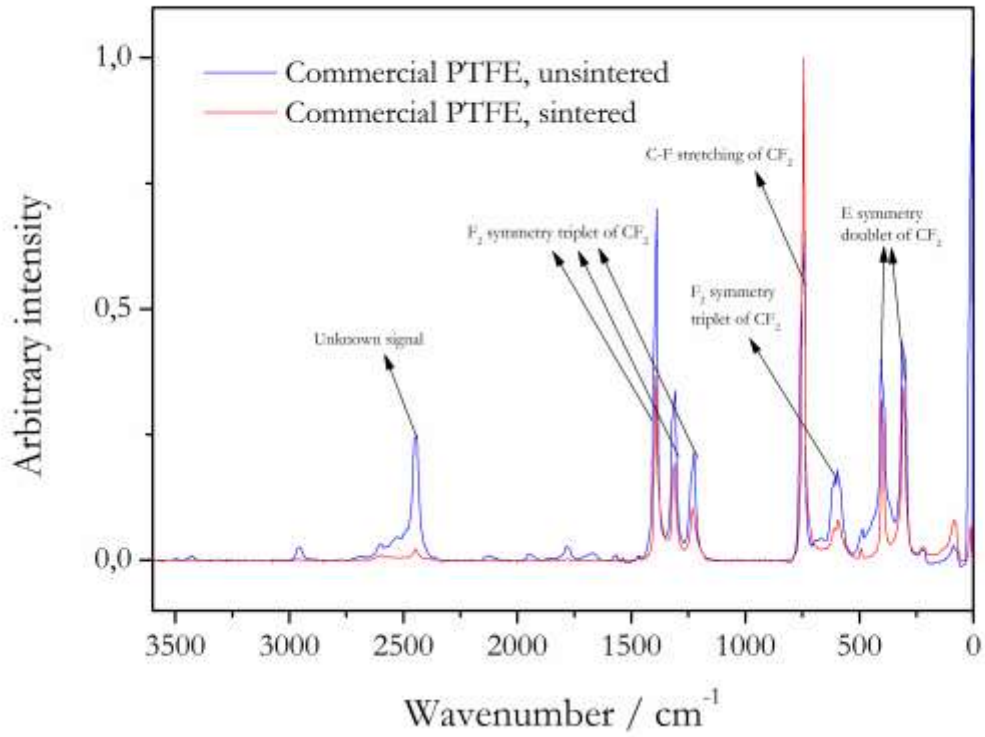

Fig. 40. Overlaid Raman spectra of commercial PTFE, before and after sintering. The sample does not undergo a structural change, but possibly a conformational one.

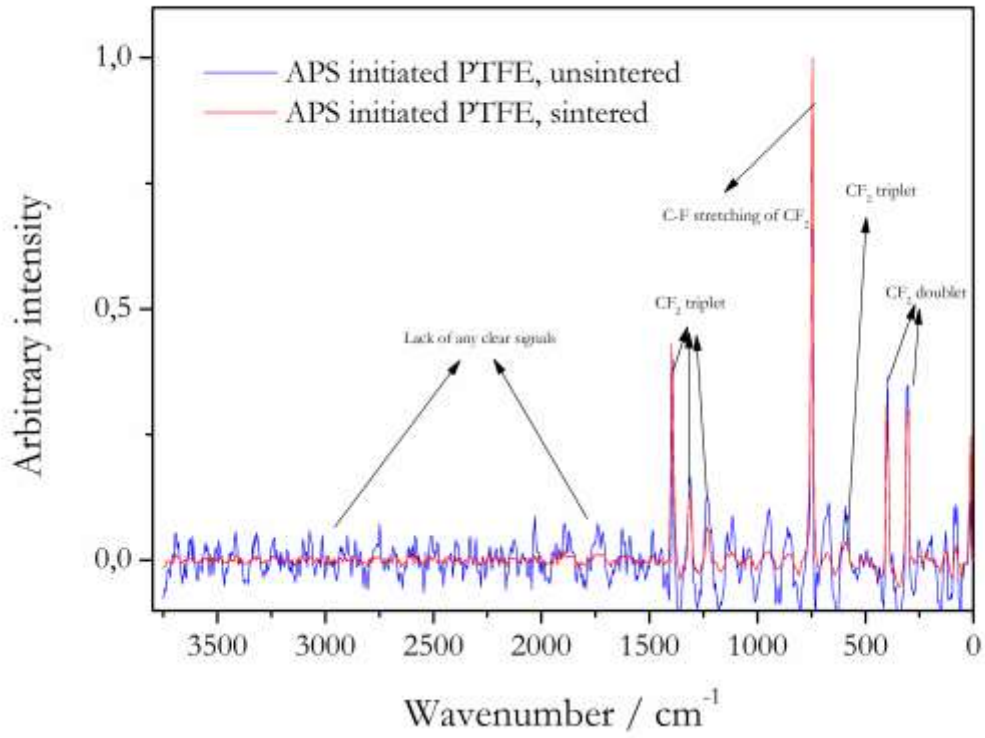

Fig. 41. Overlaid Raman spectra of APS initiated PTFE, before and after sintering. It is clear that even the sintered version of the APS initiated PTFE delivers very noisy spectra. It is difficult to discern much from this spectra, but what can be determined is that the PTFE structural peaks all seem to be unchanged. From this it can be deduced that the chains are unchanged by sintering.

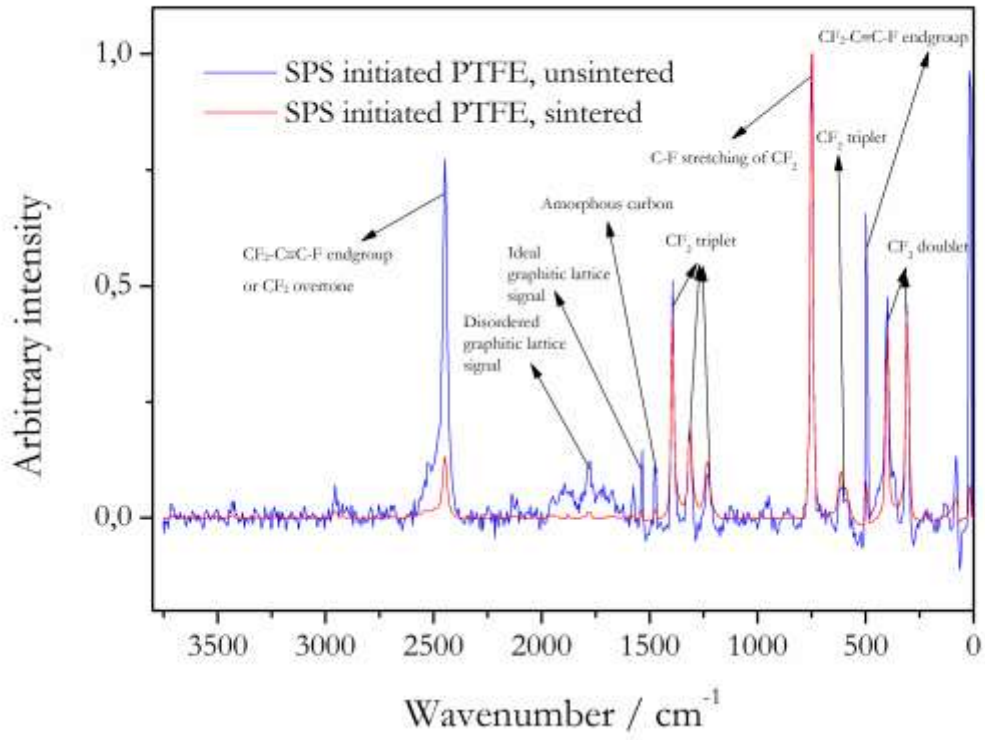

Fig. 42. Overlaid Raman spectra of SPS initiated PTFE, pre- and post-sintering. It is believed that the band at ~2450 cm^{-1} and its subsequent change post-sintering in the Raman spectra is due to conformational changes in the helical structure of PTFE.

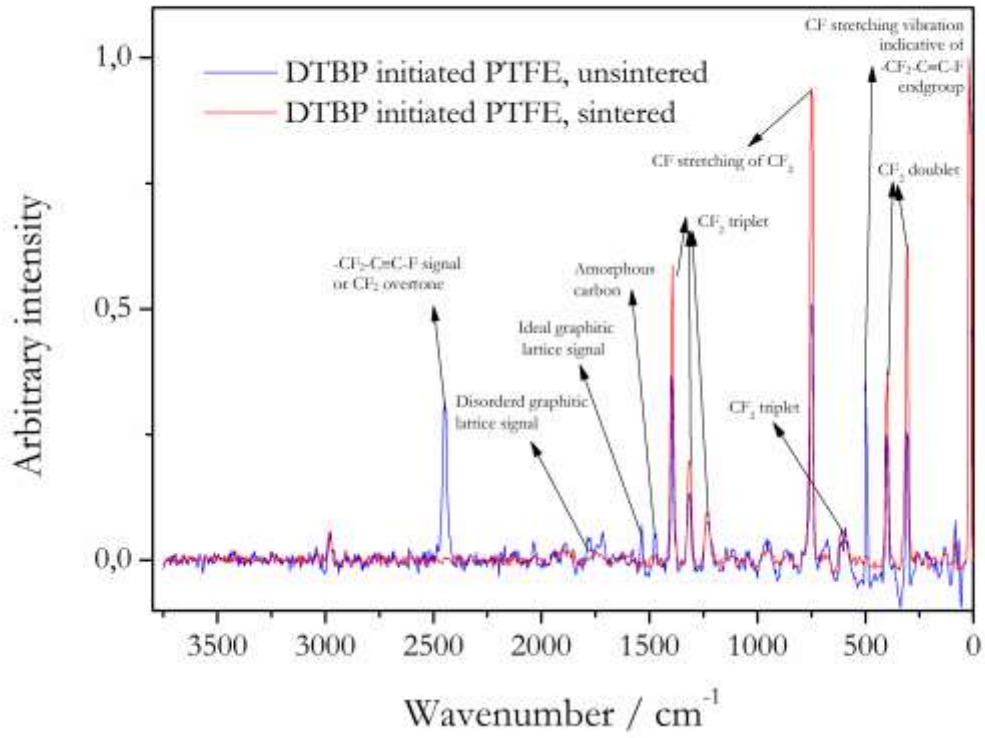

Fig. 43. Overlaid Raman spectra of DTBP initiated PTFE, pre- and post-sintering. The Raman results for the sample indicate that the polymer undergoes a conformational change during sintering, similar to the other samples.

5. TGA curves

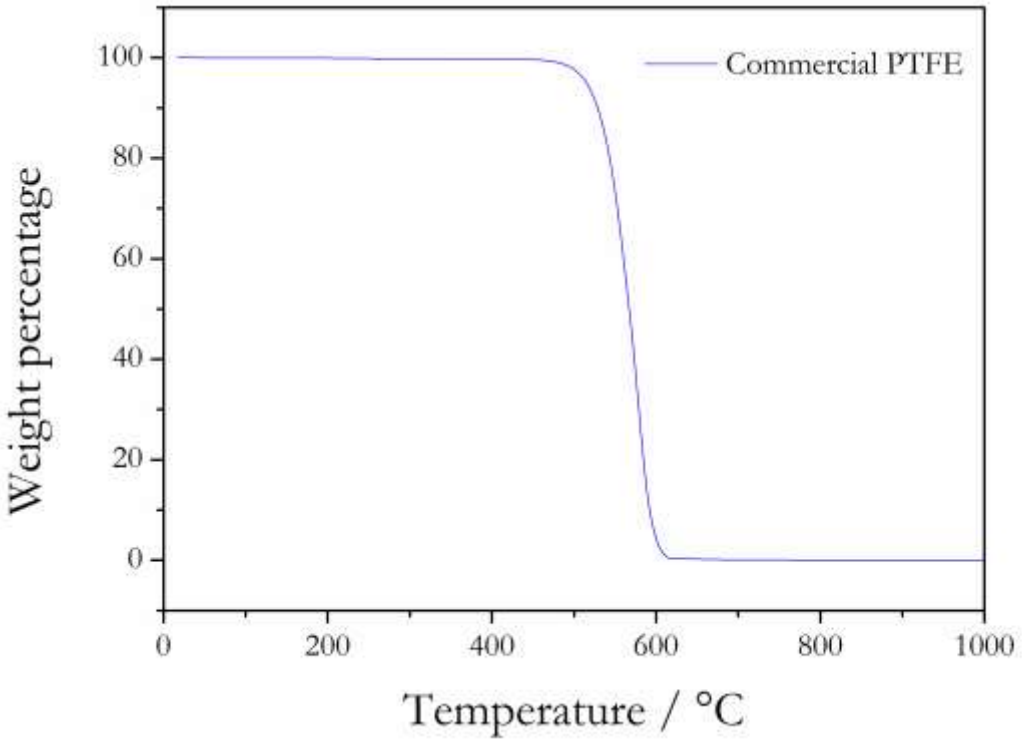

Fig. 44. TGA curve for commercial PTFE. The commercial PTFE is of a very high molecular weight and therefore only starts to decompose at very high temperatures. However, once started, this decomposition proceeds very rapidly with increasing temperature.

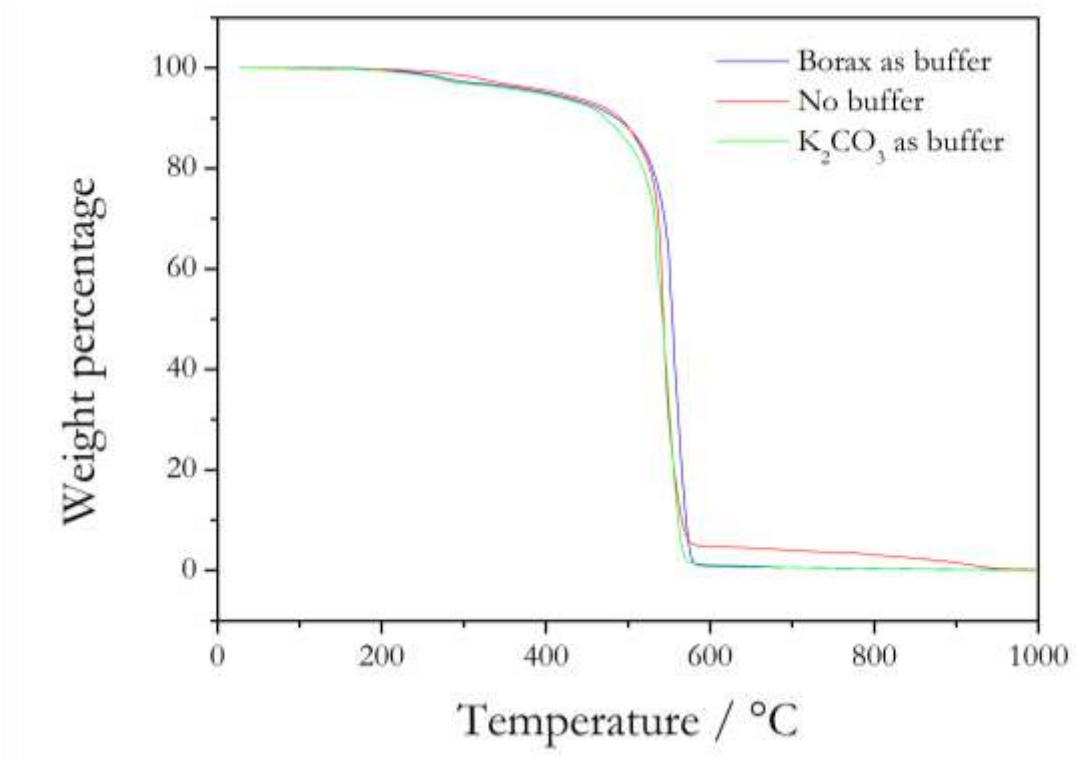

Fig. 45. TGA curves for APS initiated PTFE using different buffers. What is interesting to see is that even though the three samples all had the same amount of initiator and the same experimental conditions, they still ended up with different molecular masses. The samples that used borax and potassium carbonate as buffers had very similar molecular weights and decomposed in very similar fashions. However, the sample which had no buffer during synthesis was seemingly of a slightly higher molecular weight.

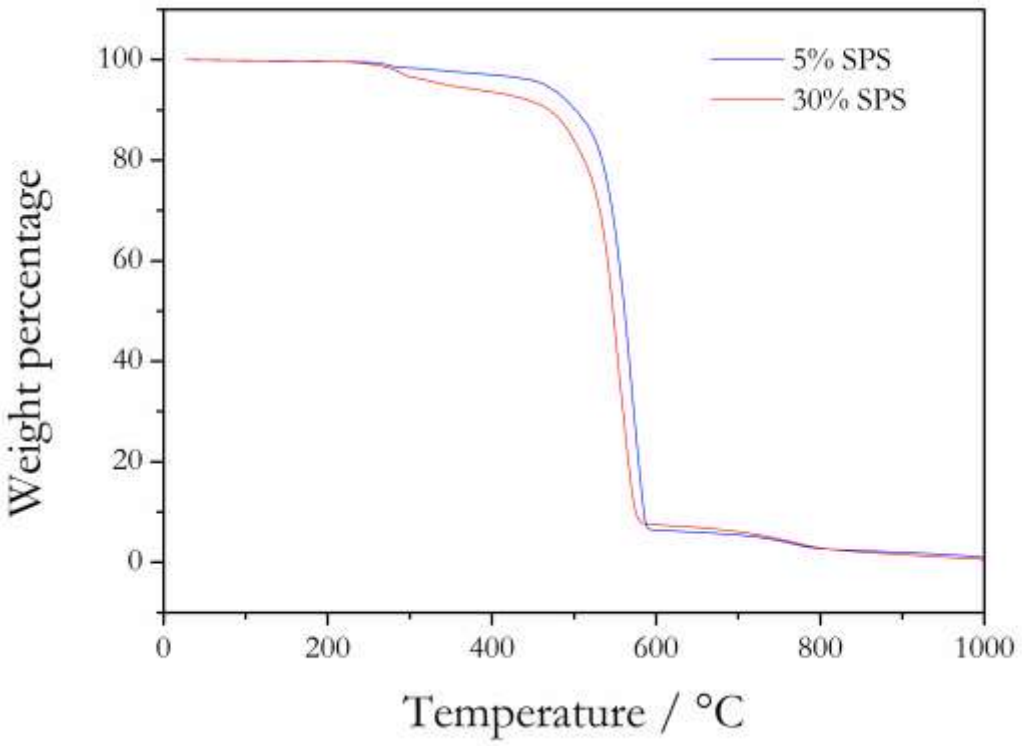

Fig. 46. TGA curves for SPS initiated PTFE using different initiator concentrations. suggest that the lower molecular weight sample has a higher polydispersity index (PDI). Lastly, it can be seen that some residual mass is left in the sample container until ~800°C. It is believed this residual mass is some form of carbon that was eliminated from the end groups and was deposited into the crucible.

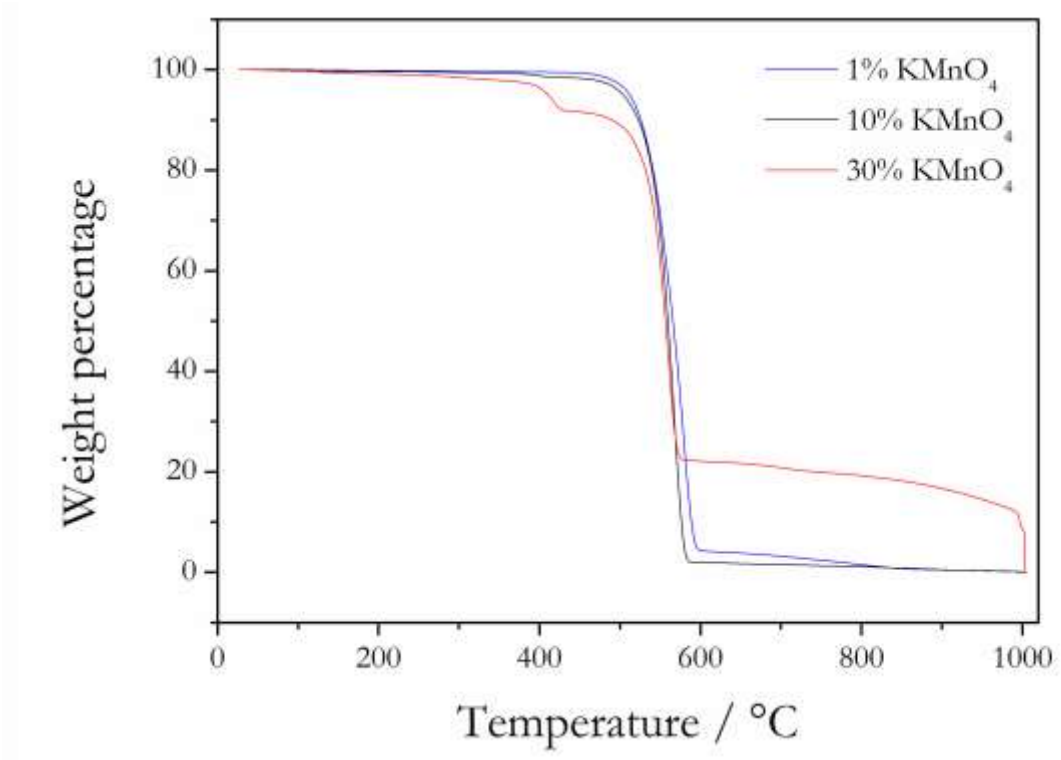

Fig. 47. TGA curves for $KMnO_4$ initiated PTFE using different initiator concentrations. The earlier onset of the decomposition can be attributed to shorter PTFE chains that evaporate before the bulk of the longer chain start to decompose. The residual mass can be attributed to amorphous carbon which decomposes at 1000°C under oxygen. It is believed this amorphous carbon is deposited into the polymer matrix when the end groups are eliminated at elevated temperatures and could be responsible for the colour change seen in the sample after sintering.

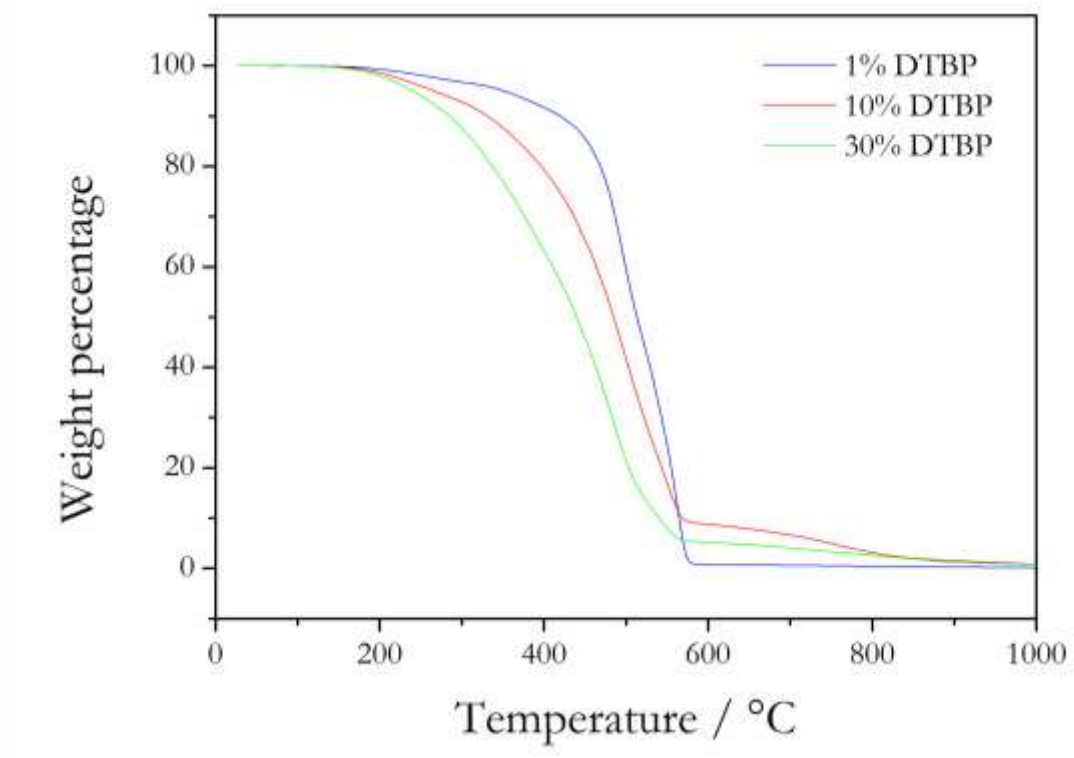

Fig. 48. Comparative TGA curves for DTBP initiated PTFE using different initiator concentrations. The earlier onset of decomposition at ~200°C shows that the DTBP initiated samples are of lower molecular weight than the $KMnO_4$ initiated samples. The decomposition also shows that these samples decomposed over a wider temperature range when compared to the other samples, indicating a higher PDI, especially in the case of the 10% and 30% initiator samples.

6. DSC curves

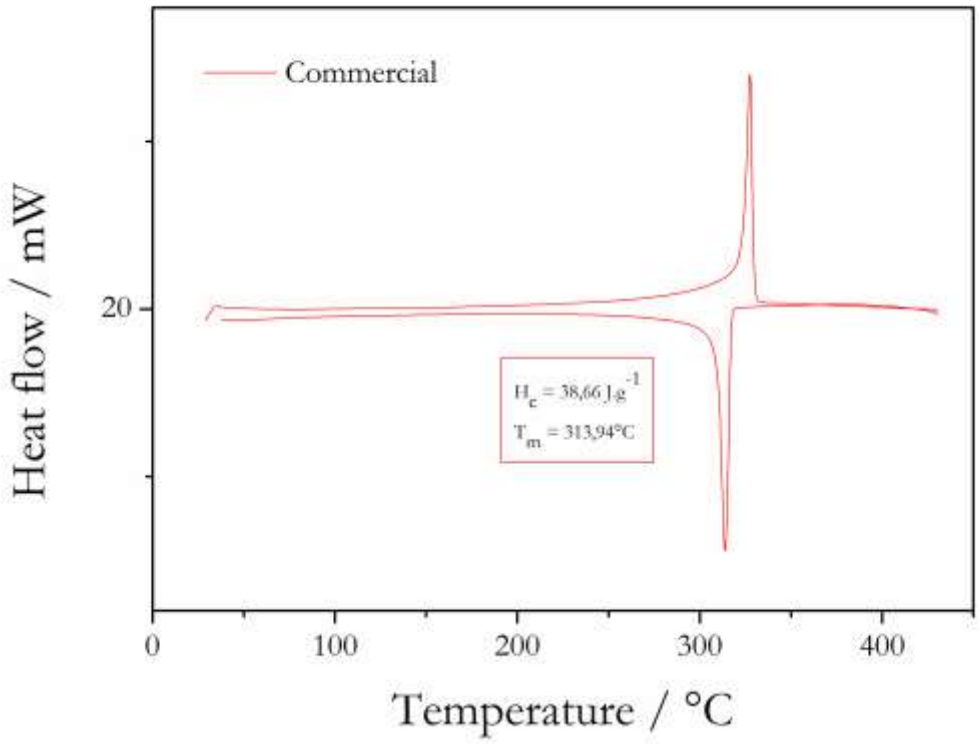

Fig. 49: DSC curve for commercial PTFE. The heat of crystallinity (H_c) was used calculate the number average molecular weight (M_n) according to Suwa's and Wiegel's methods [5]. These results for all the thermally initiated samples are tabulated in, along with the yields for the same samples.

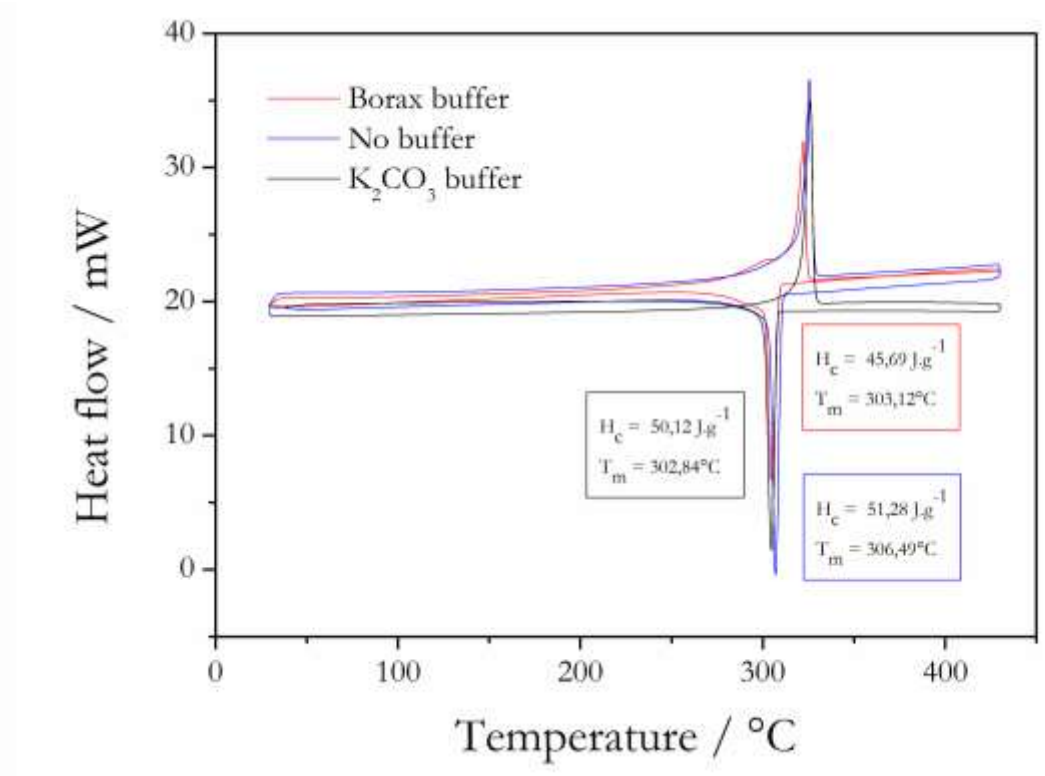

Fig. 50: DSC curves for APS initiated PTFE samples synthesised with different buffering agents. It shows that while the heat of crystallisation for the borax and potassium carbonate buffered samples are very similar, the value for the buffer-free sample is higher. The same applies to the melting point. This seems to support the TGA result which shows that the buffer-free sample is of a higher molecular weight than the samples that were synthesised with a buffering agent.

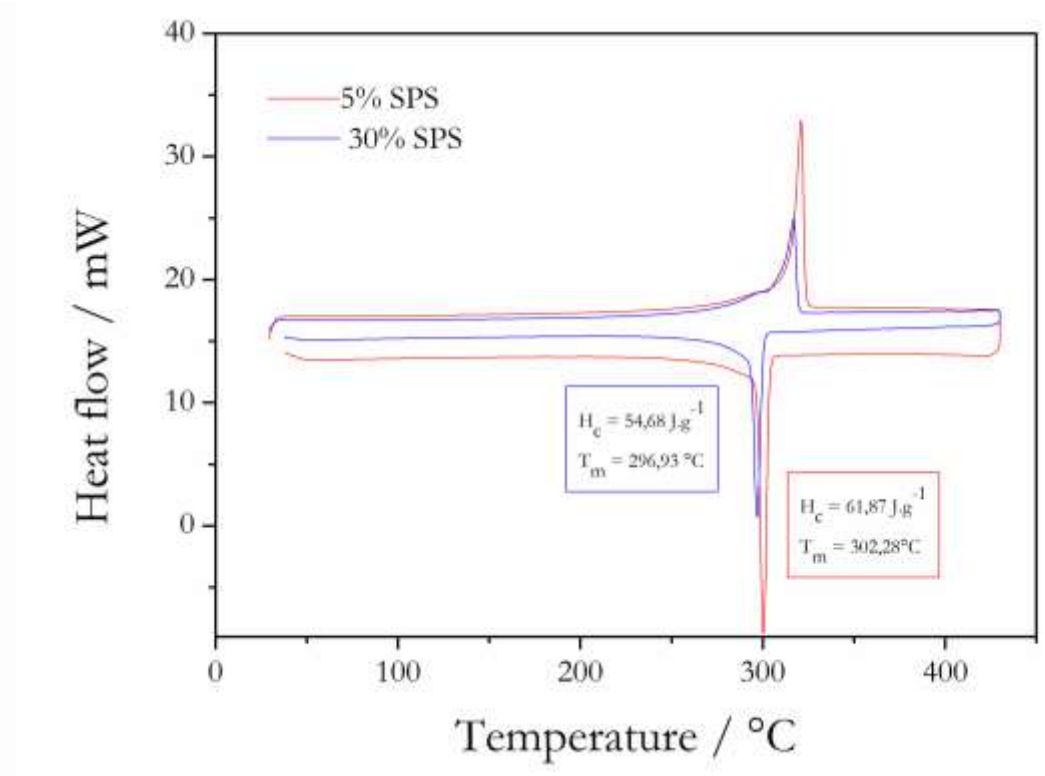

Fig. 51: DSC curves for SPS initiated PTFE. It can be seen that the crystallisation peak is smaller and broader for the lower molecular weight sample than for the higher molecular weight sample. This is completely contradictory to what was reported by Suwa *et al.*,. Therefore, it seems that Suwa's correlation is not valid for these samples, because the underlying assumption has been proved invalid. However, it should be noted that Suwa's correlation is only valid over a narrow range of values. It can also be seen that the melting temperature for the lower molecular weight sample is several degrees lower than for the higher molecular weight sample, which makes sense, because melting temperature should increase with increasing molecular weight.

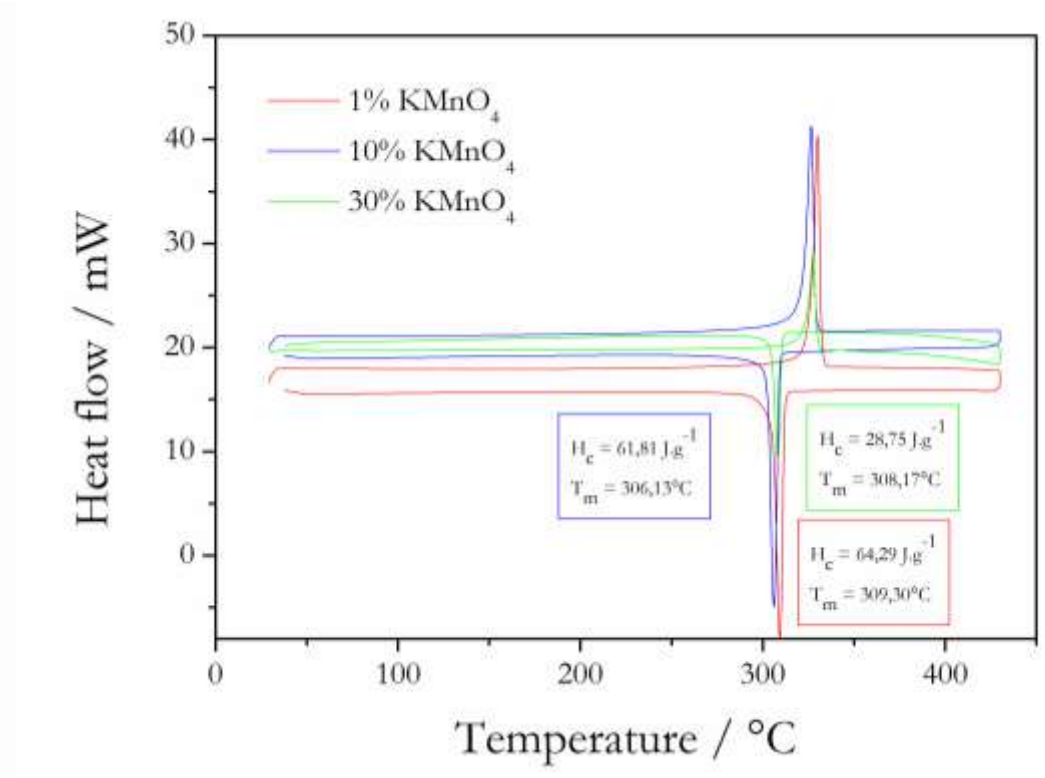

Fig. 52: DSC curves for $KMnO_4$ initiated samples. The heat of crystallisation decreases with decreasing molecular weight. It can also be seen that the lower the molecular weight, the lower the melting temperature. What is interesting is that with decreasing molecular weight, the crystallisation peaks seem to become smaller and broader, once again in direct contradiction with what was reported in the literature.

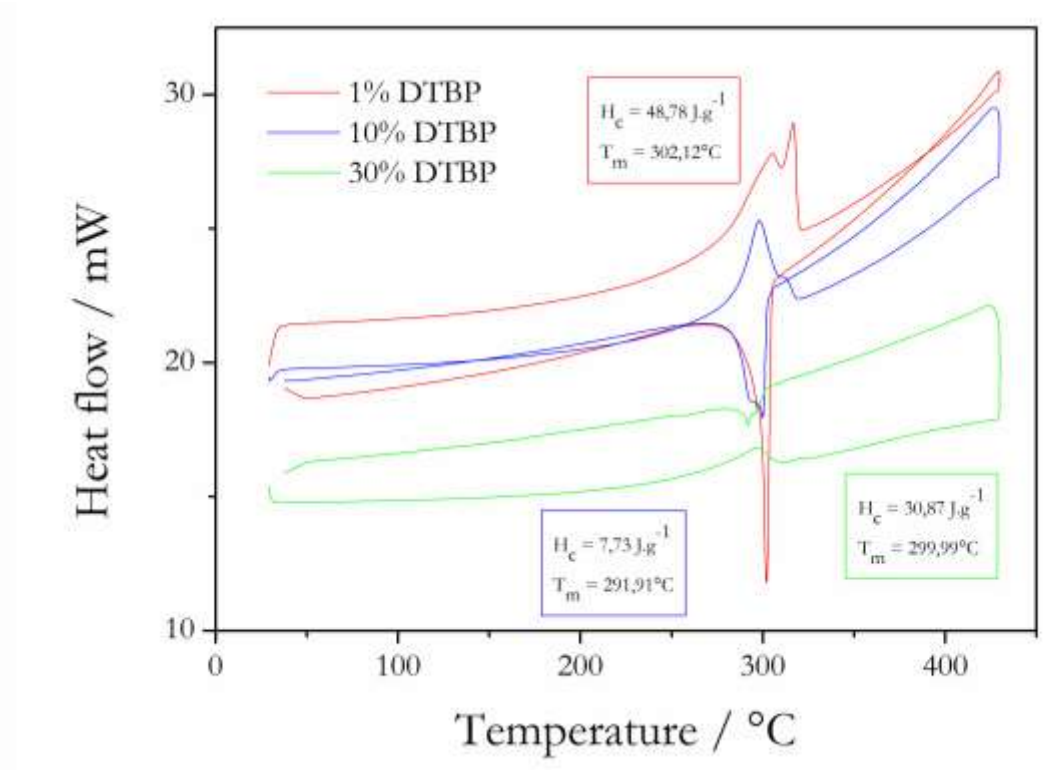

Fig. 53: DSC curves for DTBP initiated PTFE. The heat of crystallisation for the lower molecular weight sample is lower than that of the higher molecular weight sample. It can also be seen that the lower the molecular weight, the lower the melting temperature. From these curves, it is obvious that the DTBP initiator delivers lower molecular weight polymer than any of the other samples, the 30% sample being of particularly low M_n, evidenced by its very low heat of crystallisation.

Table 1: Yields and Molecular mass of thermally initiated PTFE samples.

Sample	Exp. #	Yield (mg)	Yield (%)	M_n as per Suwa's	M_n as per Wiegel's	Melting temperature

				method	method	(°C)
Commercial		n/a	n/a	2.19×10^{6}	3.65×10^{7}	313.94
1 % $KMnO_4$	20	1.9277	38.55	1.98×10^{5}	3.30×10^{6}	309.3
10 % $KMnO_4$	21	2.5783	51.57	2.83×10^{5}	4.72×10^{6}	306.13
30 % $KMnO_4$	22	1.3836	27.67	9.83×10^{6}	1.64×10^{8}	308.17
1 % DTBP	23	2.8508	57.02	1.17×10^{6}	1.95×10^{7}	302.12
10 % DTBP	24	2.8572	57.14	1.57×10^{7}	2.62×10^{8}	299.99
30 % DTBP	25	1.3836	27.67	2.60×10^{10}	4.33×10^{11}	291.91
5.5 % SPS	18	4.4068	88.136	2.32×10^{5}	3.86×10^{6}	300.28
30 % SPS	19	3.3382	66.764	4.19×10^{5}	6.99×10^{6}	296.93

7. References

1. Wavefunction, I., Spartan'06. Wavefunction, Inc.: Irvine, CA.
2. Socrates, G., Infrared and Raman characteristic group frequencies: tables and charts. 2004: John Wiley & Sons.
3. Pianca, M., et al., End groups in fluoropolymers. Journal of Fluorine Chemistry, 1999. 95(1–2): p. 71-84.
4. Moynihan, R.E., The Molecular Structure of Perfluorocarbon Polymers. Infrared Studies on Polytetrafluoroethylene1. Journal of the American Chemical Society, 1959. 81(5): p. 1045-1050.
5. Lappan, U., et al., The estimation of the molecular weight of polytetrafluoroethylene based on the heat of crystallisation. A comment on Suwa's equation. Macromolecular Materials and Engineering, 2004. 289(5): p. 420-425.